

DP-915

664519

AEC RESEARCH AND DEVELOPMENT REPORT

# HEAVY WATER MODERATED POWER REACTORS

PROGRESS REPORT  
MAY-JUNE 1964

Technical Division  
Wilmington, Delaware

RECORD

COPY

DO NOT RELEASE  
FROM FILE

TIS FILE  
RECORD COPY



ISSUED BY

*Savannah River Laboratory*

*Aiken, South Carolina*

This report was prepared as an account of Government sponsored work. Neither the United States, nor the Commission, nor any person acting on behalf of the Commission:

- A. Makes any warranty or representation, expressed or implied, with respect to the accuracy, completeness, or usefulness of the information contained in this report, or that the use of any information, apparatus, method, or process disclosed in this report may not infringe privately owned rights; or
- B. Assumes any liabilities with respect to the use of, or for damages resulting from the use of any information, apparatus, method, or process disclosed in this report.

As used in the above, "person acting on behalf of the Commission" includes any employee or contractor of the Commission, or employee of such contractor, to the extent that such employee or contractor of the Commission, or employee of such contractor prepares, disseminates, or provides access to, any information pursuant to his employment or contract with the Commission, or his employment with such contractor.

Printed in USA. Price \$1.25  
Available from the Office of Technical Services  
U. S. Department of Commerce  
Washington 25, D. C.

664579

DP-915

Reactor Technology  
(TID-4500, 31st Ed.)

HEAVY WATER MODERATED POWER REACTORS  
PROGRESS REPORT  
MAY-JUNE 1964

D. F. Babcock, Coordinator  
Power Reactor Studies  
Wilmington, Delaware

Compiled by R. R. Hood

Issue Date: July 1964

E. I. DU PONT DE NEMOURS & COMPANY  
EXPLOSIVES DEPARTMENT - ATOMIC ENERGY DIVISION  
TECHNICAL DIVISION - WILMINGTON, DELAWARE

CONTRACT AT (07-2) - 1 WITH THE  
UNITED STATES ATOMIC ENERGY COMMISSION

## ABSTRACT

The Heavy Water Components Test Reactor (HWCTR) was shut down most of May and June 1964 for repair of equipment. A D<sub>2</sub>O leak in one of the steam generators was repaired, and shaft seals were replaced on the main D<sub>2</sub>O pumps. A cladding failure occurred in an assembly of compacted UO<sub>2</sub> fuel tubes at extremely low exposure because of inadequate sealing of an end plug during fabrication of the tubes.

A technique was developed for the calculation of multi-group one-dimensional neutron density distributions by the use of heterogeneous one-group diffusion calculations.

Additional UO<sub>2</sub> fuel tubes for HWCTR irradiation tests were fabricated, and fabrication development was started on a set of UO<sub>2</sub> driver fuel tubes for the HWCTR.

An engineering study of large D<sub>2</sub>O-moderated power reactors indicated that reactors designed for liquid D<sub>2</sub>O or organic cooling are technically feasible in capacities at least as large as 8300 MW (thermal).

## CONTENTS

	<u>Page</u>
List of Tables and Figures	4
Introduction	5
Summary	5
Discussion	7
I. The Heavy Water Components Test Reactor	7
A. Reactor Operation	7
B. Pump Seals	8
C. Radiolysis of D <sub>2</sub> O	8
D. Failure Analysis of Safety Rod Guide Tubes	9
E. Zircaloy Surveillance Program	10
F. Failure Analysis of 17-4 PH Bolts in HWCTR Gas Baffle	11
G. Postirradiation Examination of Driver Fuel Tubes from First Driver Cycle	12
II. Calculation of Neutron Absorption Rates in D <sub>2</sub> O-Moderated Lattices	13
A. General	13
B. Theory	14
C. Mixed Rod Lattices - Comparison with Experiment	17
III. Reactor Fuels	19
A. General	19
B. Uranium Oxide Tubes	19
1. Fabrication of Irradiation Specimens	19
2. Oxide Driver Tubes for the HWCTR	20
3. Postirradiation Examination of Irradiation Specimens	21
4. Electron Beam Welding Facility	22
IV. Reactor Design and Evaluation Studies	22
A. Engineering Feasibility of Large Reactors	22
1. Engineering Feasibility	23
2. Description of Reactors	24
3. Development Program	25
4. Costs	25
5. Program	25
B. Advanced Converter Reactors	25
1. Reactor Descriptions	25
2. Fuel Management in the D <sub>2</sub> O-Thorium Reactor	26
Bibliography	47

LIST OF TABLES AND FIGURES

<u>Table</u>		<u>Page</u>
I	Operating Chronology of HWCTR	28
II	Operating Summary of HWCTR	28
III	Test Fuel Irradiation Data	29
IV	ZrO <sub>2</sub> Thickness and H <sub>2</sub> Content in HWCTR Rod Guide Tube No. 5	30
V	Mechanical Tests on HWCTR Rod Guide Tube No. 5	30
VI	Analysis of Mixed Lattice Element-to-Element Absorption Ratios	31
VII	THERMOS-HERESY Results for a Three-Component Mixed Lattice Supercell	31
VIII	Neutron Balance for Startup Core of D <sub>2</sub> O-Thorium Reactor	32
IX	Neutron Balance for Equilibrium Core of D <sub>2</sub> O-Thorium Reactor	33
 <u>Figure</u>		
1	Operating Power of HWCTR	34
2	Heavy Water Quality in HWCTR	35
3	Fractures in HWCTR Rod Guide Tube No. 5	36
4	HWCTR Driver Assembly No. 15, Fuel Tube No. 22	37
5	HWCTR Driver Assembly No. 11, Fuel Tube No. 48	38
6	Wigner-Seitz Cell Boundaries	39
7	Components Used in Mixed Lattice Experiments	40
8	Pin Loadings for Mixed Lattice Experiments	41
9	Flux Map in Lattice of Figure 8c	42
10	Current Field in Lattice of Figure 8c	43
11	Lattice for 1000-MWe Thorium-Fueled Heavy Water Reactor	44
12	Fuel Assembly Cross Section for 1000-MWe Thorium-Fueled Heavy Water Reactor	45
13	Composition of Fuel Charged to D <sub>2</sub> O Reactor	46

HEAVY WATER MODERATED POWER REACTORS  
PROGRESS REPORT  
MAY-JUNE 1964

INTRODUCTION

This report reviews the progress of the Du Pont development program on heavy-water-moderated power reactors. The over-all goal of the program is to advance the technology of these reactors so that they could be used in large power stations to generate electricity at fully competitive costs. Program emphasis is being placed on reactors that are cooled by liquid  $D_2O$ . The principal phases of the program are: (1) the irradiation of candidate fuels and other reactor components in the Heavy Water Components Test Reactor (HWCTR), (2) the development of low-cost fuel tubes for use in large water-cooled reactors, and (3) the technical and economic evaluation of various reactor design concepts.

SUMMARY

The HWCTR was shut down during most of the report period for repair of equipment. Shaft seals on the two main  $D_2O$  pumps were replaced after 19,000 and 13,000 hours of service, and a  $D_2O$  leak in one of the steam generators was repaired. A cladding failure occurred in an assembly of Zircaloy-clad  $UO_2$  tubes that reached an extremely low exposure (30 MWD/MTU); the failure was ascribed to inadequate sealing of an end plug during fabrication of the tubes.

Mechanical failures of Zircaloy-2 guide tubes for HWCTR safety rods (DP-905) were attributed to a combination of high tensile stresses during rod drop tests and appreciable residual stresses at the outer surface of the tubes. As a result of these failures, a program has been initiated to assess the current condition and to estimate the service life of other Zircaloy components in the HWCTR.

A technique was developed for the synthesis of multi-group one-dimensional neutron density distributions with the results of heterogeneous one-group diffusion calculations. The theory was tested numerically with the THERMOS and HERESY codes. Agreement with exact calculations was satisfactory in slab lattices, and agreement with measured rod-to-rod  $1/v$  foil absorption rate ratios was good for mixed lattices of rods that varied in blackness by a factor of 4.

Fabrication was completed on additional  $\text{UO}_2$  fuel tubes for irradiation in the HWCTR. Fabrication development was started on a set of 24  $\text{UO}_2$  driver fuel assemblies for the HWCTR. A loading procedure was developed that will enable the  $\text{UO}_2$  in these tubes to be compacted to 82% of theoretical  $\text{UO}_2$  density by vibratory compaction; however, wall thickness variations were excessive ( $>\pm 5\%$ ), and additional development is required to space the inner and outer sheath tubes more accurately during  $\text{UO}_2$  loading.

A study of the engineering feasibility of large  $\text{D}_2\text{O}$ -moderated power reactors was completed. Reactors of 3500 MW (thermal) and 8300 MW (thermal) were considered in this study, and liquid- $\text{D}_2\text{O}$ -cooled and organic-cooled designs were included. It was concluded that it is technically feasible to construct pressure tube reactors for either  $\text{D}_2\text{O}$  or organic cooling in capacities at least as large as 8300 MW. However, more development will be required for organic cooling than for  $\text{D}_2\text{O}$  cooling. The principal limitation on capacity is the space problem of arranging the coolant loops and the refueling equipment around the reactor in an efficient manner. The study is being extended to include a construction cost estimate for a nominal 1000-MWe power plant that incorporates a 3500-MW (thermal)  $\text{D}_2\text{O}$ -cooled-and-moderated reactor.



## DISCUSSION

### I. THE HEAVY WATER COMPONENTS TEST REACTOR (HWCTR)

The HWCTR is a D<sub>2</sub>O-cooled-and-moderated test reactor in which candidate fuel assemblies and other reactor components are being evaluated under conditions that are representative of large water-cooled D<sub>2</sub>O-moderated power reactors. Currently, fuel assemblies of uranium oxide (mechanically compacted in Zircaloy sheaths) and assemblies of uranium metal (coextruded with Zircaloy cladding) are being irradiated in this reactor.

#### A. REACTOR OPERATION

The reactor was shut down during most of this report period for repair of equipment, as discussed below. Near the end of the period, fuel irradiation tests were resumed at full reactor power. Operating data for the reactor are summarized in Tables I and II and in Figures 1 and 2. Irradiation tests currently in progress are summarized in Table III.

Early in the report period, modifications and repair of the gas baffle were completed (DP-905), and operation of the reactor cooling system was resumed. Excessive D<sub>2</sub>O leakage from the shaft seal of one of the main D<sub>2</sub>O pumps forced a shutdown of the system for seal replacement. After the seal was replaced, nuclear operation was resumed.

After operation of the reactor for 2 days at a maximum power of 12 MW, the No. 2 steam generator developed a D<sub>2</sub>O leak of about 200 pounds per day. The leak was in a tube in the innermost row adjacent to a sparger that introduces the H<sub>2</sub>O feedwater into the steam generator. A tube in a similar position failed earlier in the No. 1 steam generator (DP-895). The cause of the failure is not known yet. An attempt to remove a section of the leaking tube for examination was unsuccessful; therefore, the tube was plugged at each end. Further efforts to examine the tube will be made during the next scheduled shutdown of the reactor.

While the steam generator was being repaired, the shaft seal in the other D<sub>2</sub>O pump was replaced. The new seal operated only a few hours before excessive inleakage of water from the seal supply system developed. The carbon throttle bushing was discovered to be severely damaged, presumably from a small piece of foreign material in the seal. A second seal was installed and performed satisfactorily.

Subsequent to the steam generator repairs, the reactor was operated for about 2 days, then was shut down because of a cladding failure in a recently charged irradiation assembly of Zircaloy-clad uranium oxide tubes. This assembly had reached an exposure of only 30 MWD/MTU\*. Inspection results are presented in Section III.

Nuclear operation of the reactor was resumed on June 18, and the reactor was operated at maximum power (42 MW) for the remainder of the month. The power level is limited by a maximum allowable temperature of 580°C in the driver fuel tubes (DP-905).

#### B. PUMP SEALS

As mentioned above, the shaft seals on both of the main D<sub>2</sub>O pumps were replaced during this report period. The service life of the original seals was good, viz., 19,000 hours on one pump and 13,000 hours on the other. In each instance, the seals were replaced not because of sudden failure but rather because of gradually increasing and erratic D<sub>2</sub>O leakage. Examination of the seals revealed circumferential grooves in the bronze and tungsten carbide faces. The grooves in the bronze face ranged up to 0.007 inch deep, while those in the tungsten carbide face were a maximum of 0.001 inch deep. A circumferential groove about 0.009 inch deep and 0.060 inch wide formed on the shaft sleeve of one seal under the O-ring that makes the seal between the tungsten carbide face and the shaft sleeve. It is thought that this groove was worn by either the "Viton"\*\*\* A O-ring or the anti-extrusion ring adjacent to the O-ring. New shaft sleeves were installed in the pumps when the seals were replaced, and design revisions are under study.

#### C. RADIOLYSIS OF D<sub>2</sub>O

The rate of D<sub>2</sub>O decomposition by radiolysis in the HWCTR is estimated from blanket gas analyses to be negligibly low. During a period of 878 MWD of continuous operation in January 1964, the estimated D<sub>2</sub>O decomposition was less than 3 grams.

\* Megawatt-days per metric ton of uranium.

\*\*"Viton" is DuPont's trademark for fluoroelastomer.

Under normal operating conditions, deuterium gas is added to the pressurizing blanket gas (helium) of the HWCTR in sufficient amounts to maintain about 20 cc of  $D_2$  (STP) per kg of  $D_2O$ . The purpose is to remove oxygen from the  $D_2O$ . Under these conditions, the oxygen concentration in the  $D_2O$  is 0.005 cc or less (STP) per kg of  $D_2O$ . Since there is no recombiner for  $D_2$  and  $O_2$  in the blanket gas system, the concentrations of the gases in the  $D_2O$  represent the steady state conditions resulting from decomposition and recombination in the irradiation field. The consumption of deuterium gas is almost completely that amount required to make up the leakage from the gas system; therefore, this consumption provides no basis for an estimate of the net decomposition of  $D_2O$ . However, the loss of oxygen from the gas system does represent an upper limit on the decomposition. During the above-mentioned operating period, about 29,000 ft<sup>3</sup> (STP) of helium containing 2 ppm of oxygen by volume was lost from the reactor. This loss of oxygen is 0.07 gram-mole, which is equivalent to a net  $D_2O$  decomposition of 3 grams.

#### D. FAILURE ANALYSIS OF SAFETY ROD GUIDE TUBES

It was reported in DP-905 that all six of the Zircaloy-2 guide tubes for HWCTR safety rods were replaced after structural failures of the tubes were discovered. Subsequent metallurgical examination of one of the tubes revealed that the failures were caused by a combination of excessive tensile stresses during safety rod drop tests and appreciable residual stresses at the outer surface of the tubes. Contributing factors were (1) an abrupt change in guide tube diameter in the region of maximum stress, (2) high hydrogen content resulting from tube fabrication and accelerated corrosion, and (3) radially oriented platelets of zirconium hydride. These conclusions are discussed further in the following paragraphs.

The diameters of the HWCTR guide tubes are reduced 0.060 inch for a distance of 3 feet at their lower end to produce hydraulic deceleration of the safety rods as they fall into the reactor (Figure 1 of DP-905). The decelerative force causes significant but undetermined stresses in the guide tubes. Safety rod drop tests are made during each reactor startup to verify proper functioning of the rods. During the 2-year life of the guide tubes, they were subjected to about 300 drop tests (strain cycles) at temperatures of 25 to 250°C. The stresses experienced by the tubes during the strain cycles were superposed on relatively high residual stresses. Unirradiated samples of the tubing exhibited circumferential tensile stresses of 13,000 to 28,000 psi at

the outer surface. The hydrogen content of the unirradiated tubing also was abnormally high, viz., 45 to 70 ppm, as a result of etching and autoclaving problems during tube fabrication.

Visual examination of Guide Tube No. 5, the most severely damaged of the six, revealed that the initial failure was longitudinal cracking. This was evidenced by the apparent age of the longitudinal cracks and the irregular path of a transverse crack (Figure 3). Approximately 1/2 inch of the main longitudinal crack and several other longitudinal cracks at the transverse crack were bright blue, which indicated that they were several months old. The remaining cracks, including the transverse one, were a bright metallic grey and were obviously fresh. The inner surface of the tube contained many minor score marks, but no indentations from possible impact of the safety rod were observed at the diameter transition.

This guide tube exhibited a thick film of zirconium oxide and a high hydrogen content. The film thickness was a maximum of 0.0003 inch, which corresponds to a weight gain of 110 mg/dm<sup>2</sup>. The hydrogen content was estimated metallographically at 125 to 300 ppm, with a high fraction of the hydride platelets oriented radially. More complete data are shown in Table IV. On the basis of ex-reactor corrosion data on Zircaloy-2, the expected corrosion during the lifetime of the guide tube (6000 hours at 200°C) is as follows: a weight gain of 10 mg/dm<sup>2</sup>, a film thickness of  $3 \times 10^{-5}$  in., and a hydrogen pickup of 30 ppm. By comparison, the data in Table IV indicate an apparent three- to tenfold increase in corrosion because of the neutron flux. No increase in the hydrogen pickup fraction is apparent beyond the 50% expected for HWCTR coolant conditions (very low O<sub>2</sub> content and a small hydrogen partial pressure).

Collapse tests on ring sections of the guide tube indicated substantial effects of irradiation and/or hydride content on ductility as shown in Table V.

#### E. ZIRCALOY SURVEILLANCE PROGRAM

A program has been initiated to assess the current condition and to estimate the remaining life of Zircaloy components in the HWCTR. Concern about the serviceability of these components resulted from the safety-rod guide-tube failures and from the observation in the guide tubes of increased corrosion and hydrogen content, adverse hydride orientations, irradiation-induced loss of ductility, and

high residual tensile stresses. The components listed below will be examined as they become available. Work on the driver housing and the guide tubes is already in progress. The program includes the tests described in Section ID, above, as well as vacuum extraction analyses for hydrogen concentration, hydraulic burst tests for strength and ductility, and X-ray diffraction measurements of preferred orientation on unirradiated samples.

HWCTR Components Proposed for  
Postirradiation Examination

<u>Component</u>	<u>Neutron Exposure, &gt;1 Mev, nvt</u>
Driver outer housing	$1.4 \times 10^{20}$
Safety rod guide tubes	$6.8 \times 10^{19}$
Other driver or fuel housings	$\sim 2.4 \times 10^{20}$
Control rod guide tubes	$\sim 10^{20}$
Target support tubes	$1.2 \times 10^{20}$
Corrosion coupons	?

F. FAILURE ANALYSIS OF 17-4 PH BOLTS IN HWCTR GAS BAFFLE

It was reported in DP-905 that repairs to a stilling baffle in the HWCTR reactor vessel were necessitated by the discovery that anchor bolts for the baffle had failed in service. Inspections revealed four failures of the eight 5/8-inch-diameter bolts that joined the gas baffle to its support legs. During removal, repairs, and modification to the baffle support system, several failures of 3/4-inch-diameter bolts were discovered. The 3/4-inch bolts failed adjacent to the first engaged thread; the 5/8-inch bolts failed in the first or second thread on the shank. Bolt specifications called for 17-4 PH stainless steel in the H1100 condition. Initial bolt stresses were unknown because no torque limit was specified during installation. Thermal stresses in the bolts during HWCTR operation were calculated to be approximately 30,000 psi. Metallurgical examinations revealed that the 3/4-inch bolts failed by stress corrosion because of improper heat treatment; the 5/8-inch bolts probably failed because of low-ductility rupture from over-stressing.

The repairs and modifications to the baffle support system included carefully prepared and installed bolts. The 5/8-inch replacement bolts contained rolled threads and were machined from "Inconel"\* X in the AMS-5667-F heat treatment.

\*"Inconel" is the trademark of International Nickel Co.

The bolts were inspected for hardness and finish. The 3/4-inch replacement bolts were machined from tempered AISI 4140 steel (ASTM No. 193-62T) and were similarly inspected. Installation procedures specified lubrication, design stress, and a torque limit.

G. POSTIRRADIATION EXAMINATION OF DRIVER FUEL TUBES FROM FIRST DRIVER CYCLE

Results of the postirradiation examination of two U-Zr driver fuel tubes from the first HWCTR driver cycle were reported in DP-905. After these results were published, some of the electronic components of the machine that was used to measure the outside diameters of the tubes were discovered to be faulty. New electronic components of proven reliability were procured, and the outside diameters of the tubes were remeasured. The volume changes were recalculated on the basis of these new data. The results of the latest inspection are presented in the following paragraphs. These results supersede those in DP-905.

The driver tubes contain fuel cores of U<sup>235</sup> (93% enrichment) alloyed with zirconium; the total uranium concentration is 9.3 wt %. The tubes were fabricated by coextrusion in Zircaloy-2 sheaths. Driver fuel tube No. 22 was irradiated to a maximum fission burnup of 1.89 atom % at a time-averaged maximum metal temperature of 498°C. The outside diameter of the tube decreased 0.007 inch (0.3%) over a section 18 to 33 inches from the top and increased about 0.005 inch (0.2%) over a section 60 to 78 inches from the top. Maximum cladding strain, calculated on the basis of the maximum increase in outside diameter, was 0.17%. The inside diameter decreased an average of about 0.008 inch (0.4%), and the length increased 3/8 inch. The maximum volume increase was 3.4%. Plots of the OD, ID, volume change, and exposure are shown in Figure 4.

At the time of its final inspection, driver fuel tube No. 48 had been irradiated to a maximum fission burnup of 1.80 atom % at a time-averaged maximum metal temperature of 485°C. Changes in the outside diameter of the fuel tube varied from a 0.4% decrease to a 0.1% increase. The maximum cladding strain, calculated on the basis of the maximum increase in outside diameter, was less than 0.1%. The inside diameter decreased an average of 0.6%, and the length increased 7/16 inch. The maximum volume increase was 3.2%. Plots of the OD, ID, volume change, and exposure are shown in Figure 5.

The plots of outside diameter in Figures 4 and 5 represent the average of continuous longitudinal scans taken every 22-1/2 degrees around each of the tubes. The azimuthal variation in diameter of each tube was less than 0.002 inch over the entire tube length, indicating that there was no appreciable ovalness. The maximum volume increases were much less than were predicted for fuel of this composition under the stated conditions of burnup and temperatures; however, the volume changes shown in Figures 4 and 5 were calculated on the basis of diameter changes only. If the increases in length of the tubes were taken into account in the calculations, volume changes would be about 0.5% higher than is indicated in the plots.

None of the components of either driver assembly showed any sign of damage due to irradiation or from mechanical causes. After inspection, samples of each fuel tube were set aside for metallographic and chemical analysis.

## II. CALCULATION OF NEUTRON ABSORPTION RATES IN D<sub>2</sub>O-MODERATED LATTICES

### A. GENERAL

In DP-905, experimental results for bucklings and neutron density ratios in several "mixed" lattices with D<sub>2</sub>O moderator were presented. Analysis of these experiments by the "source-sink" theory of Feinberg<sup>(1)</sup> and Galanin<sup>(2)</sup> (as encoded in the IBM-704 program, HERESY<sup>(3)</sup>) is being carried out. The iterated "source-sink" method developed below has proven to be superior, in ease of application, to the iterated two-dimensional diffusion theory scheme previously described in DP-905.

The "source-sink" technique is simple in principle. Each lattice component is examined individually as an isolated cylindrical assembly in an infinite sea of moderator. The thermal neutron flux distribution due to one fission in this single element is called the "source" Green's function; the depression of the thermal flux due to one absorption in this element is the "sink" Green's function. The ratio of thermal absorptions in the element to the thermal flux at the surface of the element is the "sink-strength",  $1/\gamma$ . A mixed lattice is considered to be a composite of individual elements; because the neutron diffusion equations are linear, superposition applies. Therefore, the resultant thermal flux in the composite lattice is the sum of the source-minus-sink Green's functions for each assembly, multiplied by the emission and absorption rates appropriate to each assembly. Since the Green's functions refer to an infinite sea of moderator, HERESY calculations always refer to a fully reflected pile;

that is, an infinite amount of pure moderator surrounds the finite lattice. In practice, a ring of strongly absorbing poison rods is placed around the finite lattice to mock up a bare lattice.

Unfortunately, the theory assumes an a priori knowledge of the thermal neutron spectrum, since the diffusion process is described in terms of one "thermal" group of neutrons. In fact, the "sink strength" is normally considered a rod parameter which may be obtained from single rod experiments<sup>(4,5)</sup>. However, a proper reduction of the Boltzmann equation to the equation considered in source-sink theory would include a dependence of the "rod parameters" on their environment. An iterative method is presented for determining the appropriate thermal neutron spectra.

## B. THEORY

Consider the Boltzmann equation in the diffusion approximation:

$$\begin{aligned}
 -\nabla_{\underline{1}}(E)\nabla\phi(\underline{r},E) + \Sigma_{a_{\underline{1}}}(E)\phi(\underline{r},E) &= q(\underline{r},E) + S_{\underline{1}}\phi \\
 S_{\underline{1}}\phi &= \int_0^{E^*} dE' [\Sigma_{\underline{1}}(E' \rightarrow E) - \Sigma_{s_{\underline{1}}}(E)\delta(E-E')] \phi(\underline{r},E')
 \end{aligned}
 \tag{1}$$

where the subscript  $\underline{1}$  denotes a homogeneous spatial region, and  $q(\underline{r},E)$  is the slowing down source past a "thermal" cutoff energy,  $E^*$ . The cutoff energy is chosen to lie within the domain of validity of slowing down theory; since there is no up-scattering past  $E^*$ , the energy-transfer cross section obeys the normalization condition of Equation (2):

$$\int_0^{E^*} dE \Sigma(E' \rightarrow E) = \Sigma_s(E')
 \tag{2}$$

The observation that fuel rods represent small regions of high thermal absorption cross section leads to the "small-source", or "source-sink", delta function characterization:

$$\begin{aligned}
 \Sigma_{a_{f_k}}(E)\phi(\underline{r},E) &= \delta(\underline{r} - \underline{r}_k) \bar{\Sigma}_{a_{f_k}}(E)\phi(\underline{r}_k,E) \\
 \bar{\Sigma}_{a_{f_k}}(E) &= \frac{\int d\underline{r}\phi(\underline{r},E)}{V_k \phi(\underline{r}_k,E)} \Sigma_{a_f}(E)
 \end{aligned}
 \tag{3}$$



where  $f$  denotes "fuel", and the rods are indexed by their position  $\underline{r}_k$ . The fact that in the nonmoderating fuel  $S_f \phi = 0$  and  $D_f(E) \neq D_m(E)$  is not considered a significant perturbation of the moderator properties because of the small volume occupied by the rods.

With the fuel rods thus removed from the reactor volume, the Boltzmann equation can be written for the neutron distribution in the moderator alone:

$$\begin{aligned}
 & -D(E)\nabla^2\phi(\underline{r},E) + \Sigma_a(E)\phi(\underline{r},E) \\
 & = q(\underline{r},E) + S\phi - \sum_k \delta(\underline{r} - \underline{r}_k) \bar{\Sigma}_{a_f k}(E)\phi(\underline{r}_k,E) \quad (4)
 \end{aligned}$$

If space-energy separability of the moderator flux is assumed and if Equation (3) is integrated over energy, the following one-group, source-sink equation is obtained:

$$-\bar{D}\nabla^2\phi(\underline{r}) + \Sigma_a\phi(\underline{r}) = q(\underline{r}) - \sum_k \delta(\underline{r} - \underline{r}_k)\phi(V_k)/\gamma_k \quad (5)$$

where the term  $S\phi$  has vanished by the normalization of the energy transfer cross section, Equation (2), and

$$\begin{aligned}
 \bar{D} &= \int_0^{E^*} D_m(E)\phi_{\text{mod}}(E)dE / \int_0^{E^*} \phi_{\text{mod}}(E)dE \\
 \bar{\Sigma}_a &= \int_0^{E^*} \Sigma_{a_m}(E)\phi_{\text{mod}}(E)dE / \int_0^{E^*} \phi_{\text{mod}}(E)dE \\
 1/\gamma_k &= \int_0^{E^*} dE \Sigma_{a_f}(E) \int_{V_k} d\underline{r}\phi(\underline{r},E) / \left[ \phi(\underline{r}_k) \int_0^{E^*} dE\phi_{\text{mod}}(E) \right] \\
 1/\gamma_k &= \int_0^{E^*} dE \int_{V_k} d\underline{r} \Sigma_{a_f}(E)\phi(\underline{r},E) / \int_0^{E^*} dE\phi(\underline{r}_k,E)
 \end{aligned} \quad (6)$$

The last step follows from the assumed constancy of the moderator spectrum and the continuity of flux across the fuel-moderator interface.

It is necessary to specify a means of determining the spectrum in the moderator and in the fuel rods. To do this, the usual Wigner-Seitz boundary conditions which may be applied in uniform lattices will be generalized. From Figure 6, which shows fuel rods in a hexagonal array, it can be seen that for a lattice of identical rods (Figure 6a), symmetry considerations give the a priori knowledge that there is no net flow of neutrons across the hexagonal contours (solid lines) surrounding each rod, and this is true for all neutron velocities. The usual Wigner-Seitz approximation now simply replaces the hexagonal contour with a circular one enclosing the same area, thus reducing the problem to a one-dimensional one. The accuracy of the final result follows physically from the fact that over most of the moderator volume, the lines of constant flux (dashed curves within the  $60^\circ$  irreducible unit cell of Figure 6) closely approximate circular arcs<sup>(6)</sup>. For very small cells, Honeck<sup>(7)</sup> has shown that the Wigner-Seitz distortion of the true reflecting boundary can lead to serious error in the fuel disadvantage factor, but has also shown how to modify the boundary condition to avoid this difficulty, and still consider only a one-dimensional system.

Figure 6b indicates schematically how the situation is changed when one considers a mixed lattice; this case is a 1:1:1 interstitial arrangement of three elements in hexagonal array. For this particular example, a  $60^\circ$  sector is still the irreducible unit cell, but the a priori knowledge of the location of the reflecting boundaries (or zero normal current contours) has been lost. It is expected, however, that the hexagonal contours will be displaced in the direction of the more weakly absorbing rods since their depression of the moderator flux is less strong. Moreover, the contours will normally enclose a simply connected area about the absorbing element when reflected about the sixfold lines of symmetry, although this cannot be demonstrated a priori. Finally, one should note that the flux and zero current contours are drawn for an average (one-group) distribution; their location must be a function of neutron velocity through the cross sections (or rod blacknesses) involved. For the present, the existence of simply connected domains enclosed by contours  $C_k$  (which are independent of neutron velocity) on which the normal component of the neutron current ( $-\nabla_n \phi$ ) is zero will be assumed. If Equation (3) is integrated over such a contour, the leakage term vanishes by Green's theorem:

$$\int_{C_k} -DV^2\phi d\underline{r} = \int_{C_k} -\nabla_n \phi dS \equiv 0 \quad (7)$$

Consequently, the neutron conservation equation for the "cell" about the  $k^{\text{th}}$  rod type becomes

$$\phi(\underline{r}_k)/\gamma_k = \int_{C_k} [q(\underline{r}) - \bar{\Sigma}_a \phi(\underline{r})] d\underline{r} \quad (8)$$

With the further very good approximations that  $q(\underline{r}) = q =$  constant and  $\bar{\Sigma}_a \approx 0$ , Equation (8) yields the simple result that the "cell" area,  $A_k$ , is proportional to the absorption rate of the  $k^{\text{th}}$  rod:

$$\int_{C_k} d\underline{r} = A_k = \left(\frac{1}{q}\right) \phi(\underline{r}_k) / \gamma_k$$

This simple result makes it unnecessary to examine moderator flux maps to locate "cell" boundaries, and permits the following iterative scheme to be easily and rapidly applied: Equation (3) is solved, within an assumed set of contours  $C_k$ , by a multigroup, transport theory code (such as THERMOS<sup>(8)</sup>). The result of this calculation is a set of spectrum-averaged parameters, Equation (6), which can be fed into HERESY for solution of the source-sink equation, Equation (4). The output of HERESY specifies a set of  $A_k$  (from which  $C_k$  may be obtained); the THERMOS calculations are repeated for this set, and so on until consistency is achieved between input and output cell areas.

### C. MIXED ROD LATTICES - COMPARISON WITH EXPERIMENT

To provide an experimental verification of the calculation of reactor parameters for mixed lattices, measurements<sup>(9)</sup> of rod-to-rod  $1/v$  absorption rate ratios and lattice bucklings were made in mixed lattices composed of the elements shown in Figure 7. These elements are quite diverse, covering a range of a factor of four in blackness. The various reactor loadings are shown in Figure 8; these comprise a 2:1, a 3:1, and a 1:1:1 mixture of components with a convenient, over-all buckling.

The experimental  $1/v$  rod-to-rod neutron absorption rate ratios are shown in Table VI. In addition, the values for this quantity as calculated by the present iterative procedure are presented for each iteration. It is apparent that the agreement of calculation and experiment is markedly improved by even one iteration; furthermore, the fact that lattices of rods most nearly matched in absorption rates converge most rapidly is in itself qualitative support of the theory.

The trend of several other important quantities with cell size iteration number is shown in Table VII for the calculations of the 1:1:1 lattice of Figure 8c. Note that for the zeroth iteration, cell areas (line 2) in the THERMOS calculations were assumed equal to the geometrical (uniform lattice) areas; a rather bad mismatch of flux levels (line 4) and spectral shapes (line 3) at the cell boundaries is evident. However the HERESY calculations based on these THERMOS parameters yield a fairly good estimate of relative rod absorption rates (line 6). The cell areas based on these absorption rates (line 7) are considerably changed from the original guesses (line 2). The result of basing the THERMOS calculations on these improved cell areas is given in the second set of columns. Agreement of cell boundary spectra is now evident, and the agreement of computed and measured relative neutron densities in the fuel (Table VI) is substantially improved.

A second test of the theory was provided by a measured moderator neutron density ( $1/v$  foil activation rate) map for the lattice of Figure 8c. A map was also made with  $\text{Pu}^{239}$  pins, giving a spectral index of the moderator flux. The two foil traverses were quite similar, implying a nearly constant moderator spectral shape. This result is borne out by THERMOS calculations. A comparison of the experimental neutron density map with that computed by the iterated THERMOS-HERESY technique is shown in Figure 9. The region in the middle of the cell is plotted directly from the HERESY results; near the rods the equal flux contours become concentric with the rods, as we should expect<sup>(6)</sup>. However, since HERESY uses only the asymptotic (diffusion theory) source-sink kernels, the transport theoretic transient<sup>(7)</sup> near the strongly absorbing rods causes the measured neutron density to fall below the HERESY values. Hence, the THERMOS (transport theoretic) values of the neutron density are shown in Figure 9 (as the dashed curves) near the fuel regions only. These contours have been taken directly from the final iteration THERMOS, since presumably the level of the moderator neutron density has been established by using the converged cell area.

The moderator map also yields directly the zero current contours; the cell areas within these contours agree with those utilized in the final THERMOS iteration to within a few percent. Figure 10 displays the current vector field as determined from the final HERESY by the usual Fick's Law expression, along with the zero current contours from Figure 9. This vector field provides a graphic illustration of the Wigner-Seitz "cell" concept.

### III. REACTOR FUELS

#### A. GENERAL

Two types of Zircaloy-clad fuel elements are currently under development in the Du Pont program on  $D_2O$ -cooled power reactors: mechanically compacted tubes of uranium oxide and coextruded tubes of uranium metal. In the development of these two alternative fuels, primary attention is being given to fuel element designs and fabrication methods that offer promise of low fabrication costs when the elements are produced in the volume required for several full-scale reactors. At present, the uranium oxide tubes are receiving program emphasis pending the outcome of current irradiations of both types of fuel in the HWCTR.

In addition to the program on uranium fuels, a modest irradiation program has been initiated on thorium fuels (DP-885). The ultimate objective of this program is to develop fuel elements that would be suitable for use in  $D_2O$ -thorium breeder reactors.

#### B. URANIUM OXIDE TUBES

##### 1. Fabrication of Irradiation Specimens

Fabrication was completed on assemblies SOT-8-2 and SOT-8-3, which consist of seven pieces each of a 13-inch-long uranium oxide tube 3.650 inches in outside diameter. These assemblies will be irradiated in the HWCTR at thermal ratings ( $fkd\theta$ ) as high as 30 watts/cm and exposures as high as 30,000 MWD/MTU. The SOT-8 elements are the largest-diameter  $UO_2$  tubes that have been fabricated so far. The tubes contain  $UO_2$  enriched to 1.2%  $U^{235}$  by mechanically blending natural  $UO_2$  and 1.5% enriched  $UO_2$ . The fused and crushed  $UO_2$  was vacuum-outgassed at  $1500^\circ C$  and then crushed and sieved into fractions and blended for vibratory compaction.

To provide the irradiation test specimens, seven Zircaloy-2 sheath assemblies 54 inches long and two assemblies 48 inches long were fabricated and loaded with  $UO_2$  by vibratory compaction on a 7800-pound-thrust vibrator. The elements ranged between 83 and 84.3% of theoretical  $UO_2$  density after vibratory loading. The tubes were then swaged to 90.0 to 92.8% of theoretical density. Because of a missing shim in the swager, four of the tubes required a third swaging pass instead of the normal two passes to reach final dimensions. One of the 54-inch tubes broke in the swager at the temporary end plug weld and was rejected. The six remaining 54-inch elements were cut and

fitted with permanent plugs and end chambers to make twenty-four 13-inch-long tubes. Six 13-inch-long tubes were fabricated from the two 48-inch tubes. These thirty elements were completed except for one which leaked through a poor vent hole weld during autoclaving, causing collapse of the inner sheath when the autoclave was depressurized. The SOT-8-2 and SOT-8-3 assemblies will be made up from the 29 acceptable tubes.

These tubes were the first that were welded in a new Zircaloy welding facility designed for large-diameter tubes. Modest development was required to eliminate excessive weld overhang on the OD and ID of the elements. Welds with acceptable overhang were produced by careful control of the welding current and by the use of plug-and-ring fixtures which were designed to hold the sheath in close contact with the permanent end plug and provide a heat sink during welding.

Fabrication of fifteen SOT-6 and fifteen SOT-9  $UO_2$  tubes for assemblies SOT-6-3B, SOT-9-3, and SOT-9-2B is currently underway. These tubes are 13 inches long and 2.545 inches in outside diameter. The SOT-6 elements contain natural  $UO_2$  and are designed to operate at a thermal rating ( $fkd\theta$ ) of 30 watts/cm. The SOT-9 tubes contain 1.2% enriched  $UO_2$  obtained by mechanically blending natural  $UO_2$  and  $UO_2$  of 1.5% enrichment; they are designed to operate at a thermal rating of 40 watts/cm. Fabrication of the tubes is complete except for autoclaving and final inspection. No difficulties were experienced in fabrication except for weld failures of two temporary end plugs at swaging.

## 2. Oxide Driver Tubes for the HWCTR

Fabrication development was started with the objective of producing a set of 24 driver fuel assemblies of mechanically compacted  $UO_2$  for the HWCTR. As discussed in DP-905, oxide drivers will increase the effective utilization of the HWCTR as a fuel test facility. The conceptual design is two nested tubes consisting of a full-length (10 ft) outer tube and a three-segment inner tube spaced by ribbed washers; the  $UO_2$  will be enriched to 3.8%  $U^{235}$ \*. Dimensions of the tubes are shown below.

\*The enrichment was reported erroneously as 45%  $U^{235}$  in DP-905.

### UO<sub>2</sub> Driver Elements for the HWCTR

	<u>Dimensions, inches</u>	
	<u>Outer Tube</u>	<u>Inner Tube</u>
Clad OD	2.760	1.570
Core OD	2.700	1.510
Core ID	2.350	1.110
Clad ID	2.290	1.050
Core thickness	0.175	0.200
Core length	112	112

A prototype tube 9 feet long with an OD of 2.630 inches and a core thickness of 0.205 inch was fabricated for flow tests. This tube was fabricated by vibratory compaction only. The UO<sub>2</sub> density was 86.3% of theoretical and the wall thickness variation was ±7%. This tube is being flow tested with dummy inner tubes equipped with ribbed washers for spacing the tubes.

Vibratory compaction loading studies for the oxide drivers were made on a Zircaloy sheath assembly with an OD of 2.630 inches and a core thickness of 0.178 inch. A loading procedure was developed for obtaining UO<sub>2</sub> densities greater than 82% of theoretical. However, wall thickness variations were greater than ±5%, and development is continuing on a device to space the inner and outer sheaths more accurately during loading.

### 3. Postirradiation Examination of Irradiation Specimens

Assembly SOT-9-2, which consisted of a column of mechanically compacted UO<sub>2</sub> tubes in Zircaloy-2 sheaths, failed in the HWCTR during a power ascension on May 30. This assembly had been in the reactor only a short time, and the maximum exposure was only 30 MWD/MTU. The maximum thermal rating, which was reached just prior to detection of the failure, was estimated at about 20 watts/cm. Inspection of the assembly revealed that the failed tube was in the fifth position from the top of the column, i.e., in the region of peak neutron flux; the visible evidence of failure was a ridge caused by collapse of the inner sheath. The other six tubes were intact and apparently undamaged.

Subsequent cave examination of the failed tube disclosed three leaks: one at the weld of a bottom vent hole, a second at the circumferential weld of the inner sheath to the bottom end cap, and a third at the crest of the longitudinal ridge that formed on collapse of the inner sheath. The hole at the vent seal probably resulted from inadequate sealing techniques during fuel tube fabrication; this hole is believed to be the

cause of failure. The other two holes probably resulted from deformation associated with collapse of the inner sheath or from interference between the collapsed sheath and inner housing tube during disassembly.

Examination of cross sections of the failed element indicated that collapse of the inner sheath occurred after nuclear shutdown of the HWCTR. The  $UO_2$  experienced mild sintering that is characteristic of normal operation of these elements at 15 to 20 watts/cm; there was no evidence of abnormally high core temperatures at the point of sheath collapse. After the first indication of failure, the failed element operated steadily at its peak rating for over an hour with little additional release of activity. If the first indication of failure coincided with collapse of the sheath, some grain growth should have occurred in the  $UO_2$ .

#### 4. Electron Beam Welding Facility

An electron beam welding facility is being installed at the Savannah River Laboratory to develop welding techniques for attaching spacer ribs to the Zircaloy cladding of power reactor fuel tubes (DP-905). Installation of the 16-inch-diameter by 16-foot-long extensions to each side of the welder vacuum chamber was completed during May. Pumpdown tests showed that the entire system (approximately 64 cubic feet of volume) can be evacuated to  $0.3 \times 10^{-5}$  mm Hg in 10 minutes. Deficiencies in the drive mechanism are being corrected so that the fuel tubes can be transported smoothly beneath the electron beam. An expanding mandrel is being fabricated to hold the ribs in place during the welding operation.

When the modifications to the facility are completed, a welding program will be initiated to develop parameters for welding ribs that are 0.060 inch thick, 0.225 inch high, and 10 feet long within an empty 3.2-inch-ID Zircaloy tube. Thirty of these ribbed tubes are required as outer housings for the oxide driver assemblies of the HWCTR.

## IV. REACTOR DESIGN AND EVALUATION STUDIES

### A. ENGINEERING FEASIBILITY OF LARGE REACTORS

The Engineering Department of the Du Pont Company has undertaken for the Atomic Energy Commission a study of the engineering feasibility of large  $D_2O$ -moderated power reactors that are cooled by  $D_2O$  or an organic liquid (DP-865). This study has now been completed, and the results are summarized in the following paragraphs. A topical report on the study



is being issued<sup>(12)</sup>. The reactor sizes specified for the study were 3500 MW (thermal) and 8300 MW (thermal). Reactors of these large sizes are of particular interest because economic evaluations indicate that heavy water reactors, which have inherently large core dimensions, have their greatest competitive potential in capacities in this range.

### 1. Engineering Feasibility

It was concluded from the design study that it is technically feasible to construct D<sub>2</sub>O-moderated pressure tube reactors in capacities at least as large as 8300 MW; this conclusion applies to both liquid D<sub>2</sub>O and organic coolants. "Feasibility" means that the plants can be designed and constructed as conceived, that the construction cost will be within the range predicted in earlier Du Pont estimates, and that the plants can be operated safely and with the intended performance. However, firm design data for the new plants are not available now. More development to obtain these data will be necessary for organic cooling than for D<sub>2</sub>O cooling.

The principal limitation on the capacity of reactors of the proposed design is the space problem of arranging the coolant loops and the refueling equipment around the reactor in an efficient manner. This problem sets a practical limit of the order of 10,000 MWt on liquid-D<sub>2</sub>O-cooled reactors, based on the use of ten or eleven primary coolant loops and two on-power refueling machines. Organic-cooled reactors should have a somewhat higher capacity limit.

Current technology of pumps and steam generators probably limits the capacity of individual primary coolant loops to 600 to 900 MWt, and 900 MWt appears to be an upper limit for the foreseeable future. On-power refueling machines are probably limited by speed of operation to a capacity of about 5000 MWt per machine, and use of more than two machines does not seem feasible. The reactor structure itself has no well-defined size limitation, but the fabrication, erection, and support of the very large calandria and shield structures become progressively more difficult as size is increased. The resultant economic penalties would become unattractive at some size beyond those which have been considered.

The problems of on-power refueling were not analyzed in any detail in this study. The feasibility of building and operating machines for this purpose has been demonstrated in Canada, but reliability and safety of operation have not been well established yet. The other major questions of feasibility, which can be resolved fully only by extended

operation of a prototype plant, are the long-term integrity of zirconium-alloy pressure tubes and the maintenance of heavy water losses at acceptably low levels.

## 2. Description of Reactors

A design concept of a vertical pressure-tube reactor developed in previous Du Pont studies was further developed and applied to four heavy-water-moderated reactors, namely:

3500 Mwt - Heavy-Water-Cooled  
3500 Mwt - Organic-Cooled  
8300 Mwt - Heavy-Water-Cooled  
8300 Mwt - Organic-Cooled

The design parameters for these reactors were similar to those shown in DP-885 for 1000-MWe units. In each instance the moderator, cold and unpressurized, is contained in a vertical calandria tank, through whose tubes pass zirconium-alloy tubes containing the fuel and the hot pressurized coolant. Coolant is supplied to and discharged from the reactor through ring headers which are located above and below the calandria, and which are connected to the pressure tubes by individual 3-inch pipes. The calandrias are about 25 feet in diameter for 3500-Mwt reactors and 38 feet for the 8300-Mwt reactors.

Approximate equipment sizes and arrangements for the primary cooling loops were established. Six loops are used for the 3500-Mwt reactors, and ten larger loops of more advanced design are used for the 8300-Mwt reactors. The pumps are single-stage centrifugals with face-type mechanical shaft seals; the steam generators are vertical U-tube units with moisture separating equipment in enlarged upper sections. Extensive use is made of carbon steel in contact with heavy water and organic.

A very preliminary concept for on-power refueling was devised based on the fuel handling machine developed by Atomic Energy of Canada Ltd., for the Douglas Point Nuclear Generating Station. Other reactor auxiliary systems were considered to only a minor degree, since they raise no serious feasibility questions. Plant facilities outside of the reactor system were not considered except that the turbine-generator sizes were established.

The reactors and their primary coolant systems are housed in spherical steel containment shells which are 250 feet in diameter for the 3500-Mwt reactors and 350 feet for the 8300-Mwt reactors.

### 3. Development Program

Aside from fuel assembly development, the major areas in which mechanical development work is required are the fuel handling equipment, the pressure-tube assemblies, and joints and seals such as those for the pressure-tube closures. Each of these development items is applicable to any size reactor of the types described, but on-line refueling will probably prove economically attractive only for reactors of large size (perhaps 1500 Mwt or larger).

### 4. Costs

The particular facilities that have been examined for feasibility in this study should be no more costly to construct than the corresponding facilities on which earlier Du Pont economic studies have been based (DP-885). No cost evaluations were made in this study; therefore, the estimates of capital costs cannot be confirmed. There is some indication that unit capital cost (dollars per kilowatt) will decrease only slightly as plant size is increased in the range of sizes covered by this investigation.

### 5. Program

The next step in the study of large reactors will be the preparation of a construction cost estimate for a nominal 1000-MWe power plant that incorporates a 3500-MW (thermal) D<sub>2</sub>O-cooled-and-moderated reactor. This estimate will be useful in evaluations of the economic feasibility of such a plant and will provide a better basis for design optimization. Work has been started on the estimate.

## B. ADVANCED CONVERTER REACTORS

The Du Pont Company is assisting Oak Ridge National Laboratory (ORNL) in an evaluation of various types of advanced converter reactors. Du Pont's function is to develop for ORNL design parameters and operating characteristics for D<sub>2</sub>O-cooled-and-moderator reactors designed either for low power costs with uranium fuel or high conversion ratios with thorium fuel. The following paragraphs summarize the information transmitted by Du Pont to ORNL.

### 1. Reactor Descriptions

Design and operating parameters for two 1000-MWe D<sub>2</sub>O-moderated reactors were submitted to ORNL. Both reactors employ liquid D<sub>2</sub>O as coolant. One design is aimed at

economical operation with  $\text{UO}_2$  fuel tubes, and is essentially the reactor described in DP-885. The other reactor is designed for high-conversion operation with  $\text{ThO}_2$  fuel tubes. The thorium-fueled reactor differs from the  $\text{UO}_2$  fueled reactor in the following respects, all of which are aimed at increasing the conversion ratio.

- a. The number of fuel positions is increased from 489 to 688 to reduce the specific power and the neutron loss to  $\text{Pa}^{233}$  (Figure 11).
- b. The pressure tubes are insulated internally, rather than externally, to reduce the temperature and the thickness of the tubes (Figure 12).
- c. On-power fueling is used to maintain reactivity so that the control rod poison in the core is minimized.
- d. A blanket of 88 thorium assemblies surrounds the outermost ring of fuel assemblies to reduce neutron leakage from the core (Figure 11). Each blanket assembly contains a single tube of  $\text{ThO}_2$  of about the same dimensions as the outer fuel tube. Each blanket assembly remains in the reactor for about 2 years, at which time it produces about 0.9 MW and contains about 0.5%  $\text{U}^{233}$ .
- e. The moderator cooling system is enlarged to remove the additional heat transferred through the blanket assemblies.

## 2. Fuel Management in the $\text{D}_2\text{O}$ -Thorium Reactor

The ground rules for the ORNL study of the thorium-fueled reactors include (a) the use of  $\text{ThO}_2$  fuel, (b) the use of enriched  $\text{U}^{235}$  as the initial fissile material, (c) optimization of the fuel cycle for economics, (d) relatively cheap uranium ( $\text{U}_3\text{O}_8$  at \$8 per pound), (e) a large nuclear industry, and (f) a 30-year plant life. The following fuel cycle data are consistent with these ground rules.

### Startup Fuel Cycle

The initial fuel charge consists of  $\text{ThO}_2$  enriched with  $\text{U}^{235}$  and irradiated as a "batch" charge. The fuel contains 1.8%  $\text{U}^{235}$  in the outer 376 assemblies (buckled zone) and 2.5%  $\text{U}^{235}$  in the 312 fuel positions in the central region of the reactor (flat zone). The fuel is irradiated until the reactivity in control rods decreases to 1.0% k, the amount allotted for load following. The average exposure of the fuel in the reactor at this time is 8500 MWD/MT.

Fresh fuel assemblies containing about 2.3%  $U^{235}$  are then charged with on-power refueling equipment into the buckled and flat zones to (a) maintain the radial power distribution, and (b) maintain criticality with  $1\% k$  held in control. About 250 days after the first fuel is discharged from the reactor, fuel containing recycled uranium ( $U^{235}$  and  $U^{233}$ ) is returned to the plant. Virgin  $U^{235}$  is added to the recycled fuel so that the reactivity will be sufficient to obtain fuel exposures of at least 20,000 MWD/MT. This method of refueling (with the addition of progressively smaller amounts of  $U^{235}$ ) continues until the concentration of  $U^{233}$  returned to the reactor equals that in the spent fuel. This startup period requires about 1000 full-power days.

#### Equilibrium Fuel Cycle

Continued recycle of the uranium over the 30-year life of the reactor causes the  $U^{236}$  to build up to about 0.8%. Figure 13 shows the variation with time of the isotopic concentration of the uranium that is charged to the reactor. Because of the  $U^{236}$  buildup, the amount of  $U^{235}$  feed that is required to maintain a constant reactivity increases gradually from 0.26 to 0.41%. The average fuel exposure during the "equilibrium" period is about 22,000 MWD/MT.

#### Neutron Balance

Typical neutron balances are shown in Tables VIII and IX for the startup and equilibrium cycles. The thermal flux ratios and average thermal cross sections were obtained from THERMOS<sup>(8)</sup> calculations, and the epithermal cross sections are infinite dilution cross sections corrected for self-shielding. The resonance integral for thorium oxide was obtained from the work of Weitman<sup>(10)</sup> with  $S_{eff}/M = 0.223$  cm<sup>2</sup>/gm. The effectiveness of the interior surfaces of the nested fuel tubes was obtained from the BSQ code that was developed for uranium fuel.<sup>(11)</sup> THERMOS calculations indicate that there is very little change in the average neutron velocity in the fuel between the startup and equilibrium fuel cycles. Table VIII shows the neutron balance after the initial charge has reached an average exposure of 8000 MWD/MT. Table IX depicts the neutron balance after the reactor has operated about 2000 days, i.e., soon after the  $U^{233}$  reaches equilibrium.

TABLE I

Operating Chronology of HWCTR

May 1 - 11	Completed gas baffle repairs
11	Attained 200°C and 5 MW
12	Shut down - low driver flow
12 - 17	Cleaned driver muff screen - replaced seal, pump #1
17	Attained criticality
18	Attained 12 MW
19	Shut down - leak in #2 steam generator
19 - 29	Repaired steam generator leak - plugged one tube
29	Attained criticality
30	Attained 23 MW
31	Shut down - SOT-9-2 fuel failure
May 31 - June 6	Discharged SOT-9-2 - repaired damaged safety rod latch
June 6	Interrupted temperature ascension - low flow on SOT-6-3
6 - 9	Discharged SOT-6-3
9	Attained criticality
10	Attained 28 MW
11 - 12	Operated at 28 MW
12	Shut down - lightning strike on 13.8-kv power line
12 - 18	Replaced thrust bearing in #2 liquid loop pump
18	Attained criticality, 200°C, and 28 MW
19	Attained 38 MW
20	Attained 42 MW
20 - 30	Operated at 42 MW

TABLE II

Operating Summary of HWCTR

	<u>May</u>	<u>June</u>		
Time reactor critical, %	14.3	51.7		
Maximum power, MW	23	42		
Reactor exposure, MWD	<u>Drivers</u>	<u>Test</u>	<u>Drivers</u>	<u>Test</u>
For month	24	6	478	86
Total accumulated in Cycle H-2	905	164	1383	250
Losses				
D <sub>2</sub> O (100 mol %), lb	47		237	
% of inventory per year	0.8		4.0	
Deuterium, g	3760		3003	
Helium, scf	61,670		76,770	

TABLE III

Test Fuel Irradiation Data  
May-June 1964(a)

Reactor power 42 MW  
Coolant pressure 1200 psig  
Coolant inlet temperature 185°C  
Moderator outlet temperature 200°C

Position	Element Number	Fuel Type	Fuel Assembly Description	Starting Date	Assembly Power <sup>(b)</sup> , MW	Specific Power <sup>(c)</sup> , watts/g	Heat Flux, pcu/(hr)(ft <sup>2</sup> )	Maximum Nominal Conditions					Maximum Exposure, watt-days/g <sup>(c)</sup>	
								Outlet Temp., °C	Surface Temp., °C	Core-Clad Temp., °C	Core Temp., °C	fkde, watts/cm	Attained	Goal
37	CANDU	Oxide Rod	Five 19-rod bundles of natural UO <sub>2</sub> pellets	10-5-62	1.09	29.3	143,000	213	216	239	-	29.3	5,920	10,000
38	SOT-6-2	Oxide Tube	Seven 14" long, 2.5" OD tubes of natural UO <sub>2</sub>	12-29-63	0.485	38.1	214,000	212	234	285	-	23.3	1,435	5,500
39	3EMT-2	Metal Tube	One 36" alloyed (1.5% Mo) 3% enriched U metal tube	5-11-64	0.695	95	470,000	197	247	368	440	-	1,260	10,000
40	SOT-1-4	Oxide Tube	Seven 14" long tubes of 1.5% enriched UO <sub>2</sub>	7-13-63	0.585	68	303,000	194	232	320	-	24.1	8,030	16,000
41	-	-	-	-	-	-	-	-	-	-	-	-	-	-
42	OT-1-2	Oxide Tube	Single 1.5% enriched UO <sub>2</sub> vibratory and swaged tube	10-5-62	0.740	62	287,000	196	230	316	-	22.8	10,750	22,000
55	OT-1-7	Oxide Tube	Same as position 42	7-13-63	0.615	53.2	246,000	195	226	300	-	19.6	6,890	22,000
56	RMT-1-2	Metal Tube	Unalloyed, natural uranium 60-mil Zircaloy-clad tube	12-29-63	0.510	42.8	224,000	219	271	409	441	-	1,670	6,600
57	SMT-1-2	Metal Tube	Ten 11-1/4" alloyed (Fe,Al) natural uranium tubes	5-19-63	0.495	32.1	247,000	207	276	332	383	-	3,780	8,800
58	SOT-1-2	Oxide Tube	Same as position 40	10-5-62	0.540	55.8	249,000	193	225	297	-	19.9	13,510	25,000
59	-	-	-	-	-	-	-	-	-	-	-	-	-	-
60	SMT-1-3	Metal Tube	Five 11-1/4" alloyed (Fe,Al,Si) natural uranium tubes	7-13-63	0.430	38.3	297,000	204	295	363	424	-	3,940	8,800

(a) Data taken on June 20, 1964; exposures as of June 30, 1964.

(b) "Flow-ΔT" power calculation; does not include moderator heating (gamma and neutron absorption).

(c) These values are based on an assembly power of 1.09 times "Flow-ΔT" power to include moderator heating.

TABLE IV

ZrO<sub>2</sub> Thickness and H<sub>2</sub> Content in HWCTR Rod Guide Tube No. 5<sup>(a)</sup>

Position in Tube	Relative Neutron Flux	Coolant Temp., °C	ZrO <sub>2</sub> Thickness, 10 <sup>-3</sup> in.		Hydrogen Content, ppm	
			ID	OD	Est. from Met. Exam.	Calc. from ZrO <sub>2</sub> Data
Top	1	190-200	0.19	0.14	175	200
Above diameter transition	10	190-200	0.22	0.18	300	240
Just below diameter transition	9	190-200	0.30	0.27	300	320
Bottom	1	190-200	0.1	-(b)	125	120

(a) ZrO<sub>2</sub> film thickness values are averages of four measurements each. Calculation of hydrogen content from ZrO<sub>2</sub> data assumed solution of 50% of the hydrogen formed by corrosion because of low O<sub>2</sub> content of coolant, and the values shown include an estimate of 50 ppm for the initial hydrogen content.

(b) Too thin to measure.

TABLE V

Mechanical Tests on HWCTR Rod Guide Tube No. 5

Position in Tube	Relative Neutron Flux	Estimated Hydrogen Content, ppm	Force, lb/inch of ring length	Deflection, fractional reduction in diameter
Top	1	175-200	60 (collapsed)	>3/4
Above diameter transition	10	250-300	80-110 (fractured)	1/3
Just below diameter transition	9	300	40- 60 (fractured)	1/3
Bottom	2	125	80-110 (fractured)	2/3
	1		65 (collapsed)	>3/4



TABLE VI

Analysis of Mixed Lattice  
Element-to-Element Absorption Ratios

Iteration (a)	Lattice	Neutron Density (b)				
		I	II	III	IV	V
0	3	-	-	-	1.00	0.606
Experiment		-	-	-	1.00	0.613 ±2%
Error						1%
0	4	0.854	-	1.00	-	-
1		0.843	-	1.00	-	-
Experiment		0.828 ±2%	-	1.00	-	-
Error		1.8%				
0	5	0.853	0.761	1.00	-	-
1		0.839	0.781	1.00	-	-
Experiment		0.810 ±2%	0.768 ±2%	1.00	-	-
Error		3.5%	1.7%			

(a) An "iteration" consists of a THERMOS calculation based on the previously determined cell areas, followed by a HERESY calculation based on the  $\gamma$ 's predicted by the current THERMOS. The zeroth iteration assumes equal cell areas as the "previous HERESY".

(b) See Figure 7 for identification of component types.

TABLE VII

THERMOS-HERESY Results for a  
Three-Component Mixed Lattice Supercell

Rod Type	Iteration 0			Iteration 1		
	I	II	III	I	II	III
$V_{\text{cell}}, \text{cm}^2$	273.8	273.8	273.8	443.1	254.9	123.3
$\bar{v}(R_{\text{cell}})^{(a)}$	1.29	1.22	1.17	1.21	1.22	1.22
$\phi(R_{\text{cell}})^{(b)}$	0.76	1.48	3.24	1.47	1.36	1.43
$\gamma$	0.224	0.403	1.012	0.236	0.399	0.985
A (relative) <sup>(c)</sup>	3.61	2.06	1.00	3.41	2.04	1.00
$V_{\text{cell}}, \text{cm}^2$ <sup>(d)</sup>	443.1	254.9	123.3	434.5	259.7	127.3

(a) Average velocity at cell edges;  $\bar{v} = 1.128$  corresponds to a Maxwellian spectrum.

(b) Based on 1 n/(cm<sup>2</sup>)(sec) slowing down source.

(c) HERESY rod absorption rates.

(d) Predicted cell areas based on HERESY absorption rates.

TABLE VIII

Neutron Balance for Startup Core of D<sub>2</sub>O-Thorium Reactor  
 1000-MWe, 160 full-power days, avg exposure of 8000 MWD/MT

Neutron Absorbers	Volume, cm <sup>3</sup> /cm	Number of Atoms/cm <sup>3</sup> x 10 <sup>24</sup>	Thermal Parameters			Epithermal Parameters		Total Neutrons Absorbed
			$\sigma$ , barns	Relative Flux	Neutrons Absorbed	RI, barns	Neutrons Absorbed	
Th <sup>232</sup>	32.39	0.0201	4.594	0.100	0.3101	14.5	0.0784	0.3885
Pa <sup>233</sup>	32.39	0.000036	43.2	0.100	0.0052	550	0.0053	0.0105
U <sup>233</sup>	32.39	0.000086	355	0.100	0.1020	990	0.0227	0.1247
U <sup>234</sup>	32.39	0.000006	59.8	0.100	0.0011	672	0.0010	0.0021
U <sup>235</sup>	32.39	0.000248	392	0.100	0.3252	397	0.0263	0.3515
U <sup>236</sup>	32.39	0.000029	4.3	0.100	0.0004	288	0.0022	0.0029
Clad Zr	7.06	0.0425	0.109	0.100	0.0034	0.92	0.0023	0.0057
Inner Zr	5.21	0.0425	0.124	0.176	0.0050	0.92	0.0017	0.0067
P. T. Zr	14.88	0.0425	0.124	0.176	0.0142	0.92	0.0047	0.0189
P. T. Nb	14.88	0.00105	0.794	0.176	0.0023	8.53	0.0010	0.0033
Cool. D	54.79	0.0506	2.9x10 <sup>-4</sup>	0.116	0.0001	-	-	0.0001
Mod. D	584.07	0.06491	3.3x10 <sup>-4</sup>	0.258	0.0033	-	-	0.0032
Mod. H	584.07	0.000162	0.0243	0.258	0.0006	0.13	0.0001	0.0007
Xe	32.39	2.72x10 <sup>-9</sup>	2.36x10 <sup>6</sup>	0.100	0.0215	-	-	0.0215
Sm	32.39	1.87x10 <sup>-7</sup>	7.2x10 <sup>3</sup>	0.100	0.0045	3090	0.0002	0.0047
F. P.	32.39	0.000193	23.5	0.100	0.0158	-	0.0070	0.0228
Leakage					0.0043	-	0.0070	0.0113
Blanket					-	-	-	0.0097
Control					-	-	-	0.0112
							Total	1.0000
<u>Neutron Producers</u>					<u>Neutrons Produced</u>		<u>Neutrons Produced</u>	<u>Total Produced</u>
U <sup>233</sup>	32.39	0.000086	325	0.100	0.2345	843	0.0486	0.2831
U <sup>235</sup>	32.39	0.000248	334	0.100	0.6746	262	0.0423	0.7169
								1.0000

(a)  $\nu^{233} = 2.43$ ;  $\nu^{235} = 2.503$ ;  $\epsilon = 1.0020$

(b) Epithermal absorptions =  $NV\phi_e RI$ ;  $\phi_e = 0.083 \phi_{\text{thermal}}$

(c) The effects of the O(n, $\alpha$ ), D( $\gamma$ ,n), and D(n,2n) events, which give a net positive reactivity contribution, are neglected.

TABLE IX

Neutron Balance for Equilibrium Core of D<sub>2</sub>O-Thorium Reactor  
 1000-MWe, 2000 full-power days, avg exposure of 22,000 MWD/MT

Neutron Absorbers	Volume, cm <sup>3</sup> /cm	Number of Atoms/cm <sup>3</sup> x 10 <sup>24</sup>	Thermal Parameters			Epithermal Parameters		Total Neutrons Absorbed
			$\sigma$ , barns	Relative Flux	Neutrons Absorbed	RI, barns	Neutrons Absorbed	
Th <sup>232</sup>	32.39	0.02010	4.594	0.100	0.3031	14.5	0.0790	0.3820
Pa <sup>233</sup>	32.39	0.000035	43.2	0.100	0.0050	550	0.0053	0.0103
U <sup>233</sup>	32.39	0.000260	355	0.100	0.3029	990	0.0704	0.3733
U <sup>234</sup>	32.39	0.000083	59.8	0.100	0.0163	575	0.0131	0.0294
U <sup>235</sup>	32.39	0.000054	392	0.100	0.0695	397	0.0059	0.0754
U <sup>236</sup>	32.39	0.000085	4.3	0.100	0.0019	224	0.0083	0.0104
Clad Zr	7.06	0.0425	0.109	0.100	0.0033	0.92	0.0022	0.0055
Inner Zr	5.21	0.0425	0.124	0.176	0.0049	0.92	0.0016	0.0065
P. T. Zr	14.88	0.0425	0.124	0.176	0.0140	0.92	0.0047	0.0187
P. T. Nb	14.88	0.00105	0.794	0.176	0.0022	8.53	0.0010	0.0032
Cool. D	54.79	0.0506	2.9x10 <sup>-4</sup>	0.116	0.0001	-	-	0.0001
Mod. D	584.07	0.06491	3.3x10 <sup>-4</sup>	0.258	0.0032	-	-	0.0032
Mod. H	584.07	0.000162	0.0243	0.258	0.0007	0.131	0.0001	0.0008
Xe	32.39	2.50x10 <sup>-8</sup>	2.36x10 <sup>6</sup>	0.100	0.0194	-	-	0.0194
Sm	32.39	1.49x10 <sup>-7</sup>	7.2x10 <sup>9</sup>	0.100	0.0035	3090	0.0002	0.0037
F. P.	32.39	0.000241	23.5	0.100	0.0178	-	0.0091	0.0269
Leakage					0.0045		0.0070	0.0115
Blanket								0.0097
Control								0.0100
							Total	1.0000
<u>Neutron Producers</u>					<u>Neutrons Produced</u>		<u>Neutrons Produced</u>	<u>Total Produced</u>
U <sup>233</sup>	32.39	0.000260	325	0.100	0.6955	843	0.1510	0.8465
U <sup>235</sup>	32.39	0.000054	334	0.100	0.1441	262	0.0094	0.1535
								1.0000

(a)  $\nu^{235} = 2.43$ ;  $\nu^{233} = 2.503$ ;  $\epsilon = 1.0020$

(b) Epithermal absorptions =  $NV\phi_e RI$ ;  $\phi_e = 0.083 \phi_{\text{thermal}}$

(c) The effects of the O(n, $\alpha$ ), D( $\gamma$ ,n) and D(n,2n) events, which give a net positive reactivity contribution, are neglected.

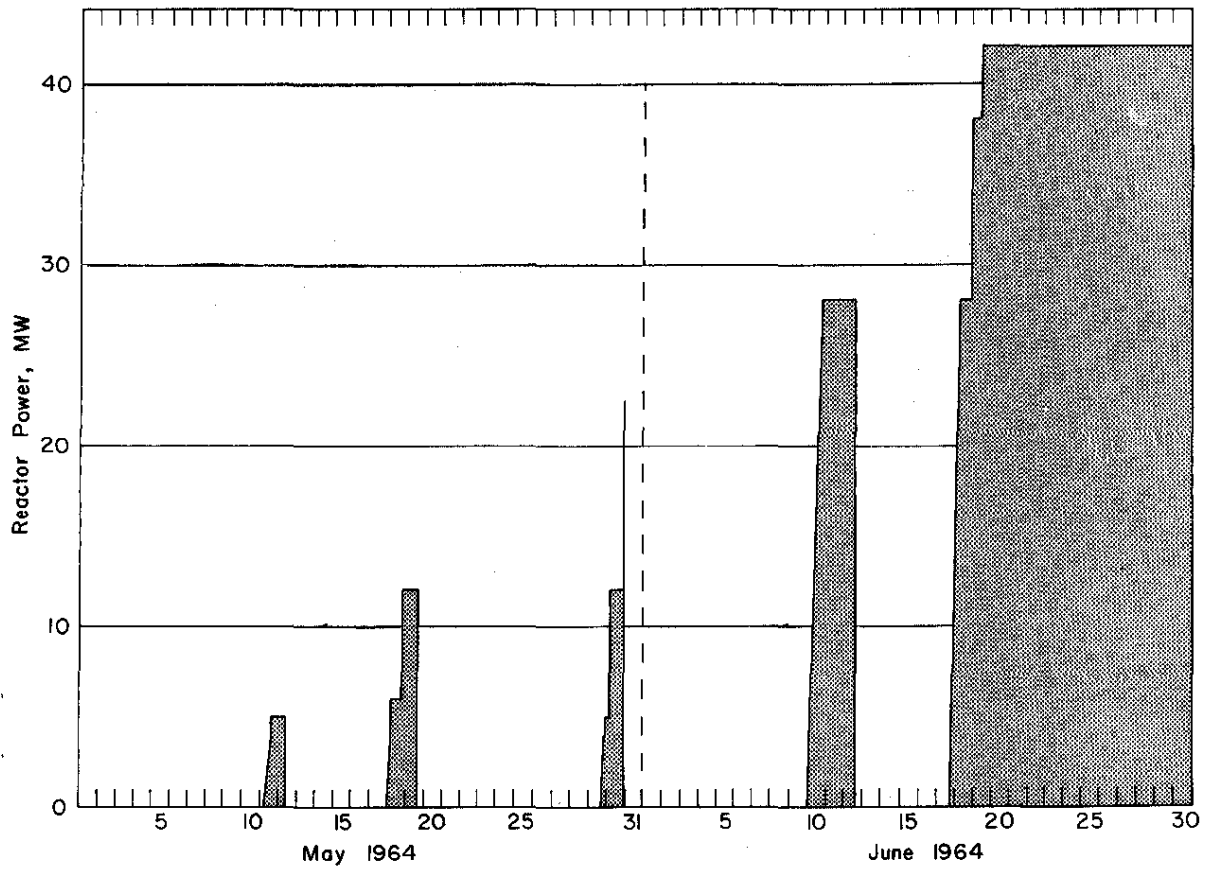


FIG. 1 OPERATING POWER OF HWCTR

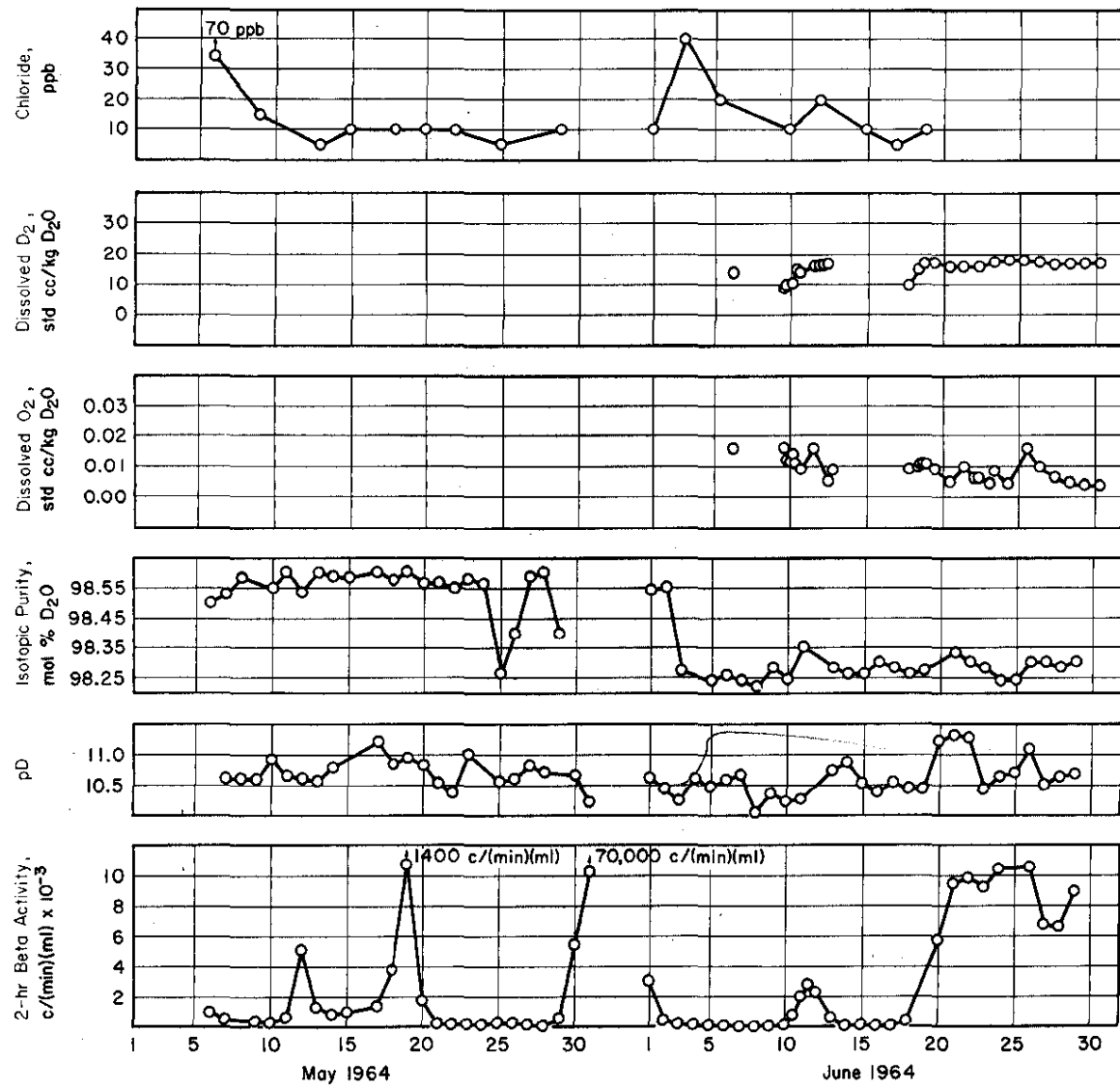
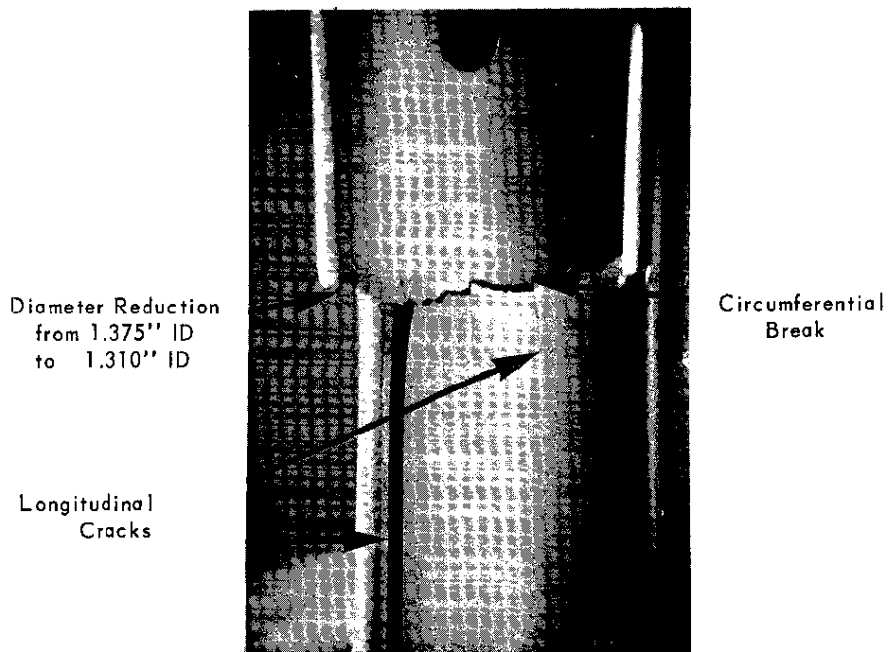


FIG. 2 HEAVY WATER QUALITY IN HWCTR



Material: Zircaloy-2, drawn and annealed

FIG. 3 FRACTURES IN SAFETY ROD GUIDE TUBE NO. 5

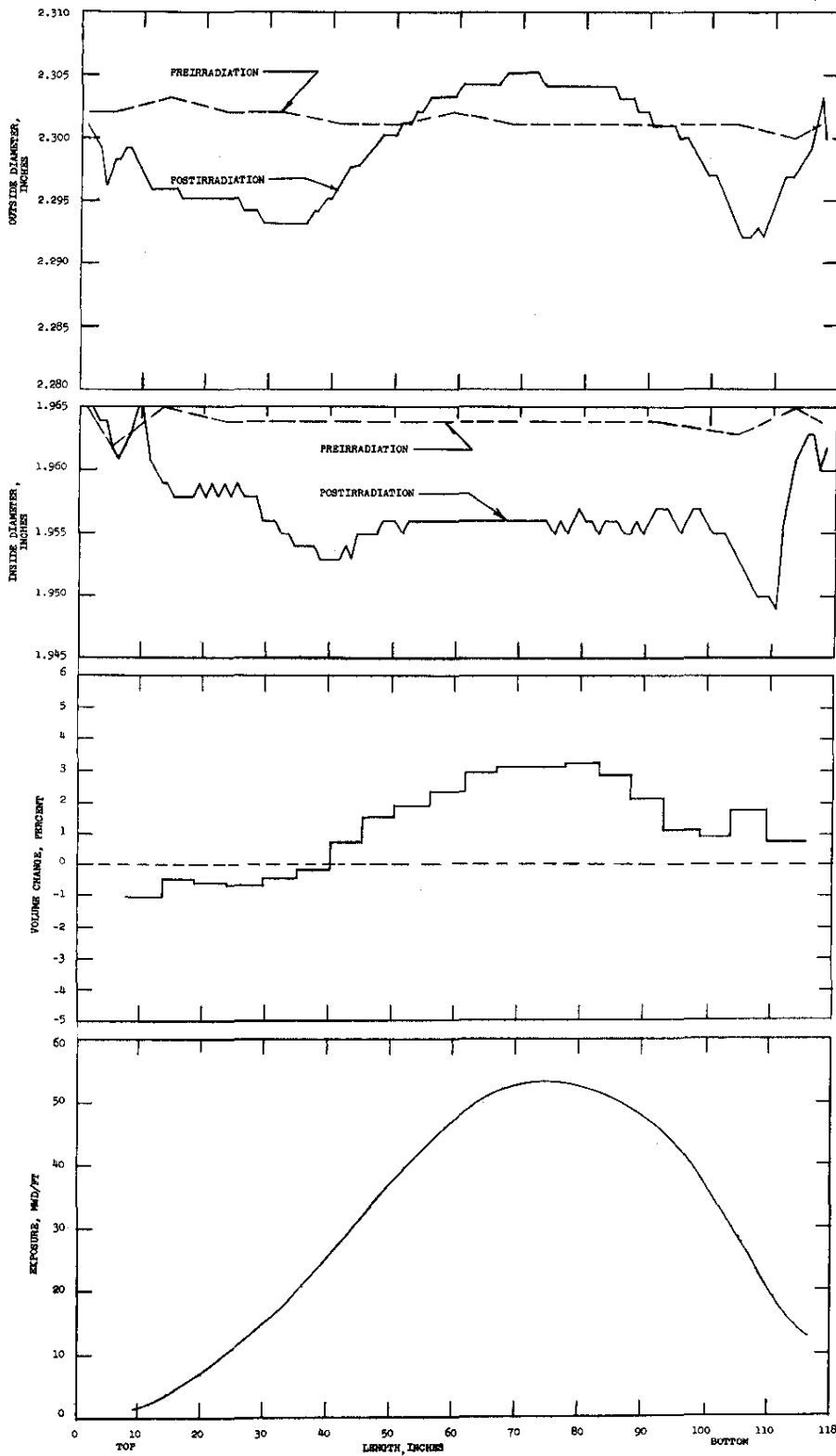


FIG. 4 HWCTR DRIVER ASSEMBLY NO. 15, FUEL TUBE NO. 22

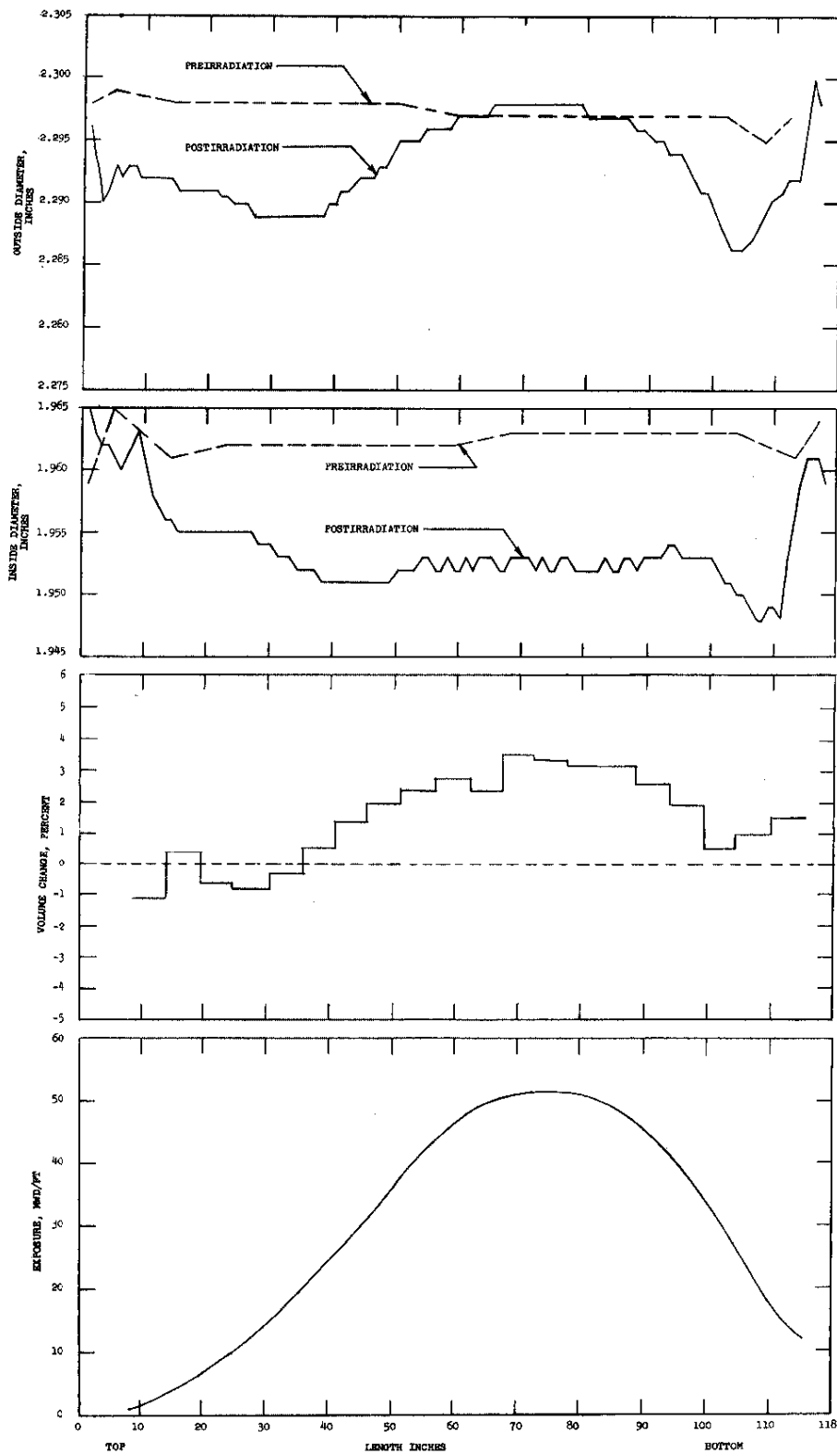
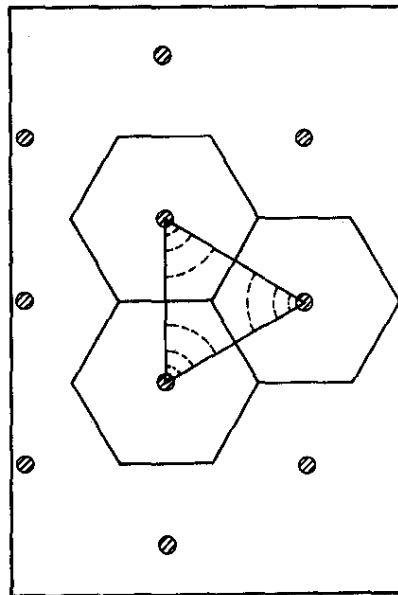
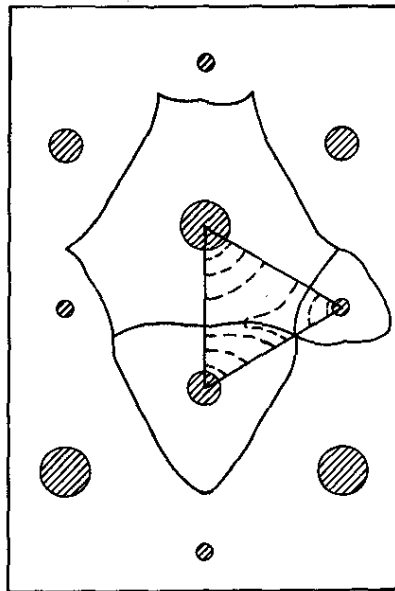


FIG. 5 HWCTR DRIVER ASSEMBLY NO. 11, FUEL TUBE NO. 48



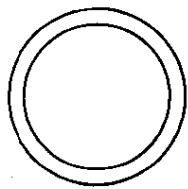


a. Uniform Lattice

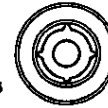


b. Mixed Lattice

FIG. 6 WIGNER-SEITZ CELL BOUNDARIES



**I.**  
**NATURAL URANIUM METAL TUBE**  
 DENSITY = 18.9 gm/cm<sup>3</sup>  
 O. D. = 3.500 inch  
 I. D. = 2.860 inch



**II.**  
**CLAD URANIUM METAL TUBE**  
 ENRICHMENT = 0.947 wt. % U-235  
 DENSITY = 18.9 gm/cm<sup>3</sup>  
 CLADDING AND INNER SUPPORT TUBE MATERIAL = 1100 ALUMINUM  
 CLAD O. D. = 1.974 inch  
 CLAD I. D. = 1.166 inch  
 BARE FUEL O. D. = 1.914 inch  
 BARE FUEL I. D. = 1.226 inch  
 SUPPORT TUBE O. D. = 0.832 inch  
 SUPPORT TUBE I. D. = 0.632 inch  
 SUPPORT TUBE RIB D. = 1.146 inch



**III.**  
**NATURAL URANIUM METAL ROD**  
 DENSITY = 18.9 gm/cm<sup>3</sup>  
 ROD O. D. = 0.998 inch  
 SHEATH MATERIAL = 1100 ALUMINUM  
 SHEATH O. D. = 1.090 inch  
 SHEATH I. D. = 1.026 inch  
 AIR BETWEEN SHEATH AND FUEL

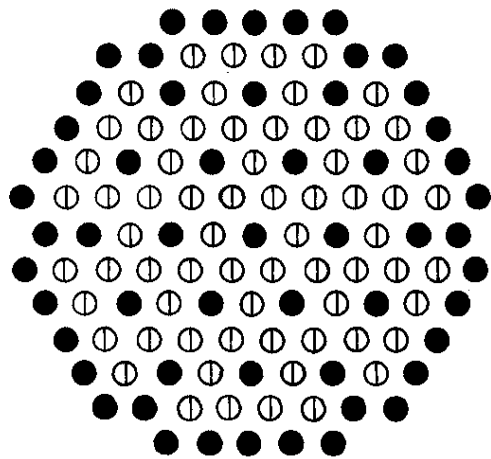


**IV.**  
**ENRICHED URANIUM-ALUM ALLOY ROD**  
 ENRICHMENT > 90 % U-235  
 5.0 wt % U-235 in ALUMINUM  
 DENSITY = 2.82 gm/cm<sup>3</sup>  
 ROD O. D. = 1.000 inch  
 SHEATH MATERIAL = 1100 ALUMINUM  
 SHEATH O. D. = 1.090 inch  
 SHEATH I. D. = 1.026 inch  
 AIR BETWEEN SHEATH AND FUEL

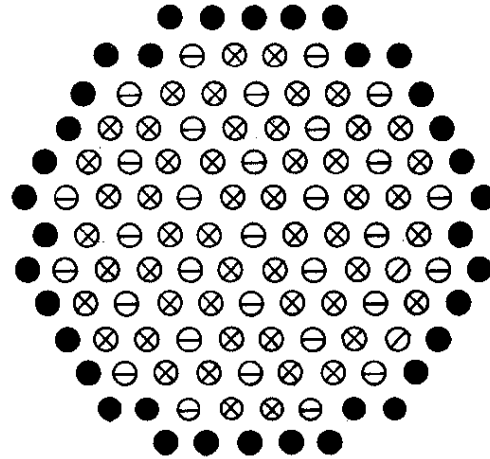


**V.**  
**NATURAL LITHIUM-ALUM ALLOY ROD**  
 LITHIUM IN ALUMINUM wt % = 4.9  
 DENSITY OF ALLOY = 2.35 gm/cm<sup>3</sup>  
 ROD O. D. = 0.930 inch  
 CLADDING & SHEATH MATERIAL = 1100 ALUM.  
 CLADDING O. D. = 1.005 inch  
 CLADDING I. D. = 0.930 inch  
 SHEATH O. D. = 1.090 inch  
 SHEATH I. D. = 1.026 inch  
 AIR BETWEEN SHEATH & CLAD ROD

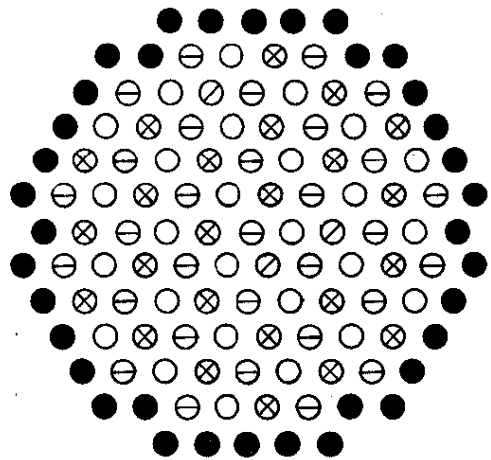
FIG. 7 COMPONENTS USED IN MIXED LATTICE EXPERIMENTS



a. PDP Loading Number 3



b. PDP Loading Number 4



c. PDP Loading Number 5

See Figure 7

- ⊖ I
- II
- ⊗ III
- ⊕ IV
- V

FIG. 8 PILE LOADINGS FOR MIXED LATTICE EXPERIMENTS

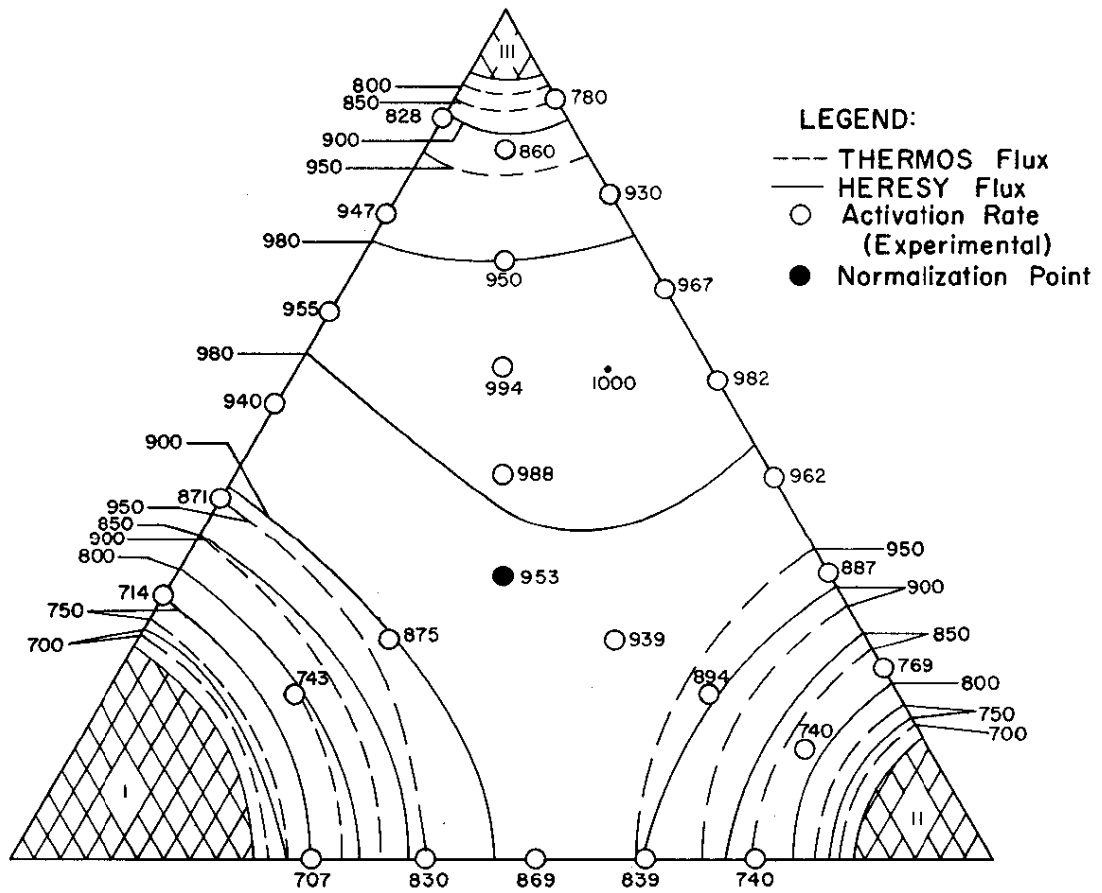


FIG. 9 FLUX MAP IN LATTICE OF FIG. 8c

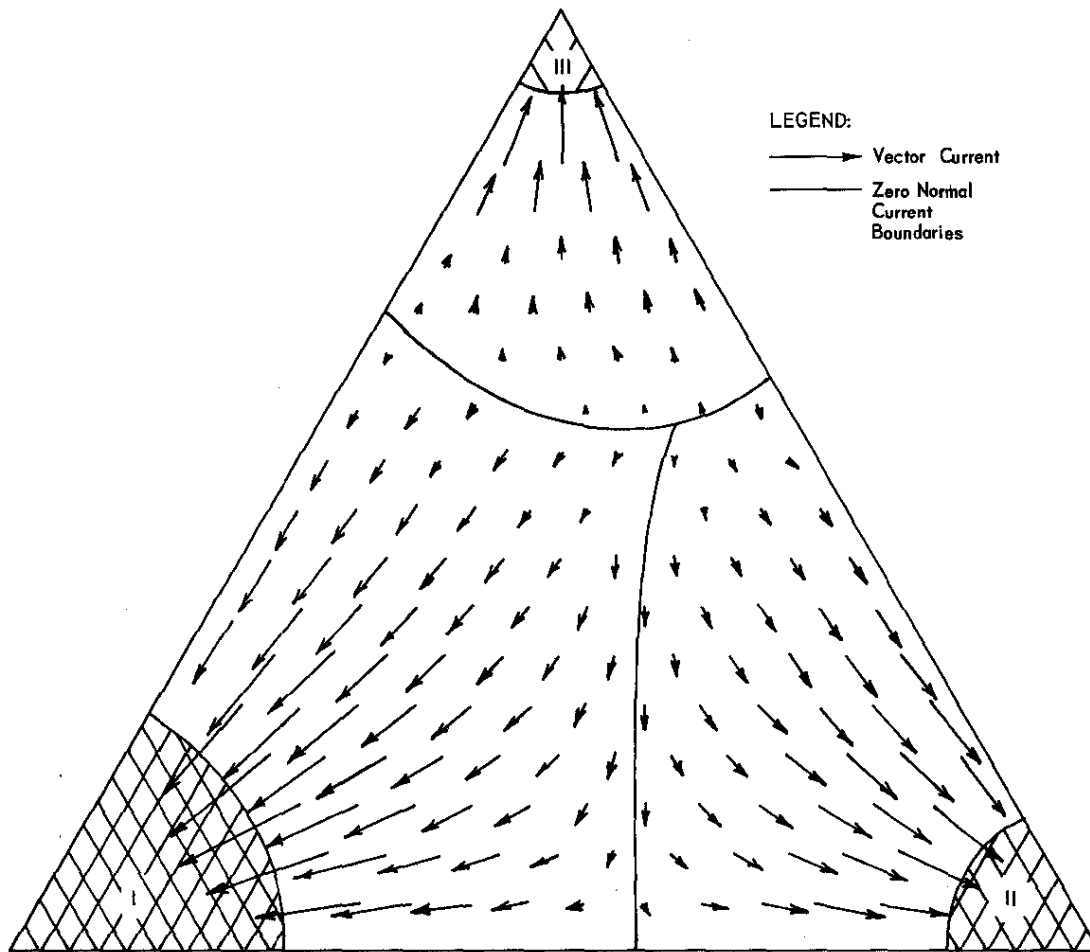


FIG. 10 CURRENT FIELD IN LATTICE OF FIG. 8c

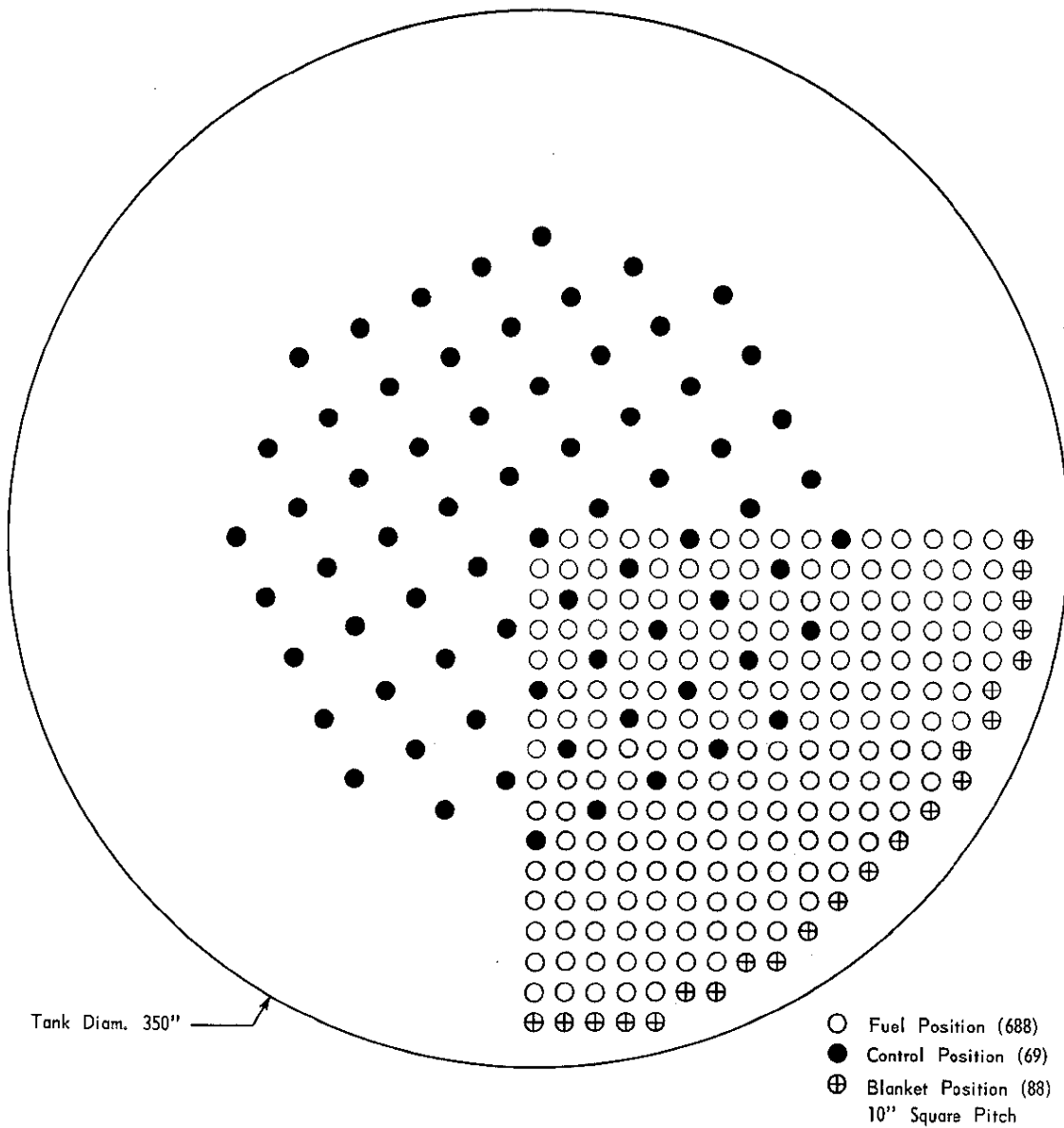
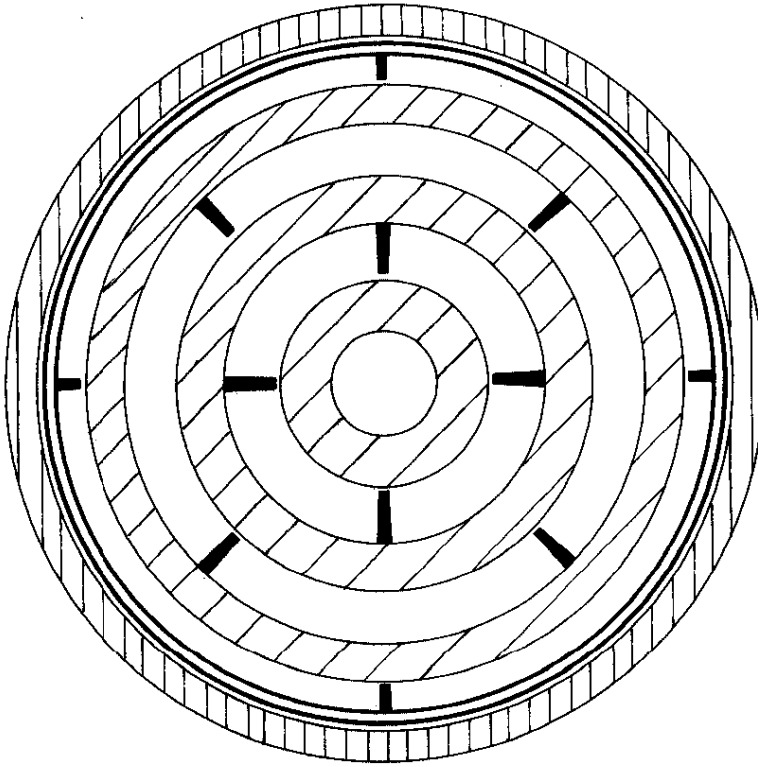


FIG. 11 LATTICE FOR 1000-MW<sub>e</sub> THORIUM-FUELED HEAVY WATER REACTOR





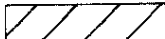
-  Zr - 2.5% Nb pressure tube
-  Zircaloy liners, ribs, and cladding
-  ThO<sub>2</sub> fuel

FIG. 12 FUEL ASSEMBLY CROSS SECTION FOR 1000-MWe THORIUM-FUELED HEAVY WATER REACTOR

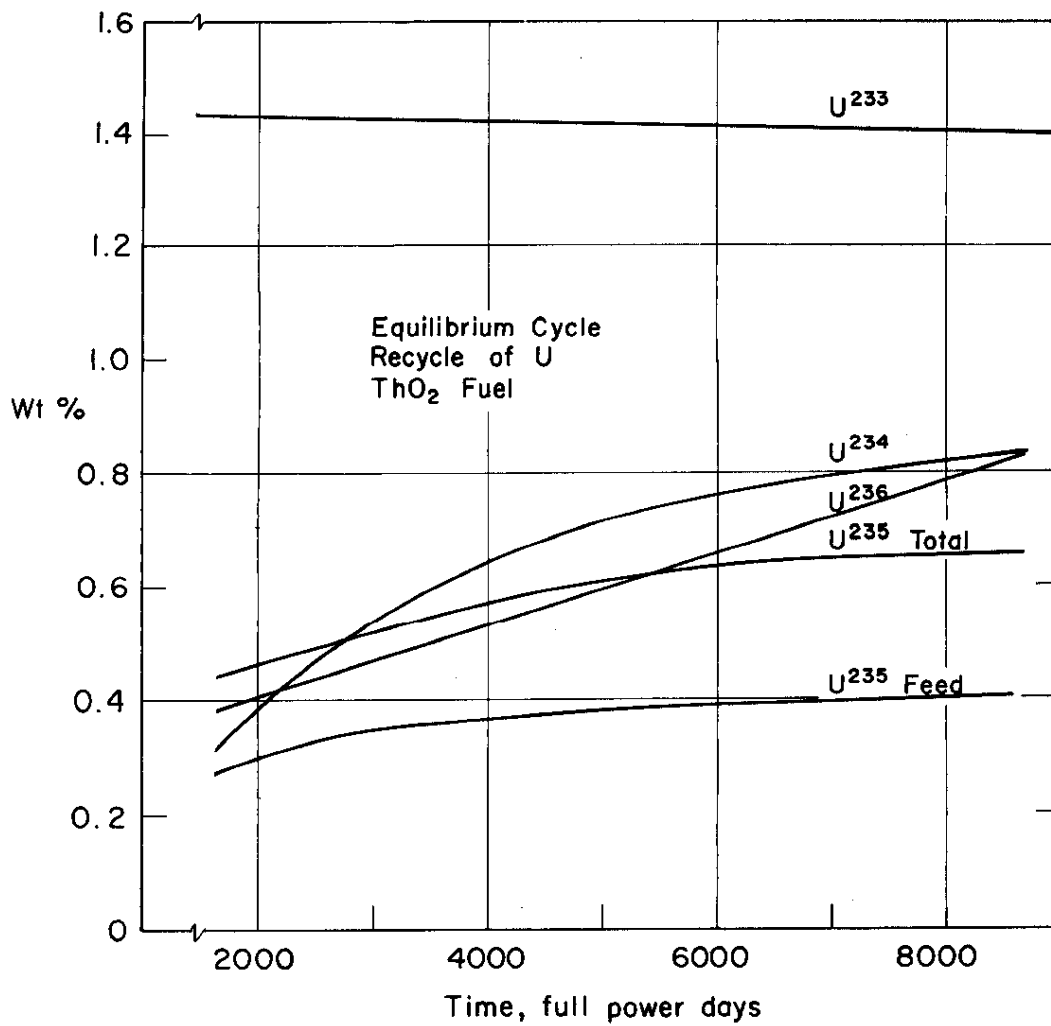


FIG. 13 COMPOSITION OF FUEL CHARGED TO D<sub>2</sub>O REACTOR



## BIBLIOGRAPHY

1. Feinberg, S. M. "Heterogeneous Methods for Calculating Reactors". Proc. Intern. Conf. Peaceful Uses Atomic Energy, Geneva, 5, 484-500 (1955). P/669
2. Galanin, A. D. "Critical Size of Heterogeneous Reactor with a Small Number of Rods". Proc. Intern. Conf. Peaceful Uses Atomic Energy, Geneva, 5, 462-65 (1955). P/663
3. Klahr, C. N., et al. Heterogeneous Reactor Calculation Method. Quarterly Progress Report No. 6, Technical Research Group 129, TRG, Inc., Syosset, N. Y. USAEC Report NYO-2678 (1960).
4. Rodeback, G. W., C. H. Skeen, and J. W. Zink. "Single Element Measurements". Trans. Am. Nucl. Soc. 2, 144-5 (1959).
5. Klahr, C. N. Heterogeneous Reactor Calculation Methods. Quarterly Progress Report No. 1, Technical Research Group 129, TRG, Inc., Syosset, N. Y. USAEC Report NYO-2673 (1959).
6. Cohen, E. Richard. "The Thermal Neutron Flux in a Square Lattice Cell". Nucl. Sci. Eng. 1 (2), 268-79 (1956).
7. Honeck, H. C. "Some Methods for Improving the Cylindrical Reflecting Boundary Condition in Cell Calculations of the Thermal Neutron Flux". Trans. Am. Nucl. Soc. 5, 350-1 (1962).
8. Honeck, H. C. THERMOS - A Thermalization Transport Theory Code for Reactor Lattice Calculations. Brookhaven National Laboratory, Upton, N. Y. USAEC Report BNL-5826 (1961).
9. Benton, F. D. and W. E. Graves. "Experimental Bucklings and Neutron-Density Ratios of D<sub>2</sub>O-Moderated Mixed Lattices". Trans. Am. Nucl. Soc. 7, 74-5 (1964).
10. Weitman, J., "The Effective Resonance Integral of Thorium Oxide Rods". Nucl. Sci. Eng. 18 (2), 246-59 (1964).
11. Driggers, F. E. "BSQ - An IBM-704 Code to Calculate Heavy Water Lattice Parameters". Heavy Water Lattices: Second Panel Report, Technical Reports Series No. 20, IAEA, Vienna (1963).
12. Large Heavy Water Moderated Power Reactors: Engineering Feasibility Study. E. I. du Pont de Nemours & Co., Engineering Department, Wilmington, Del. USAEC Report DP-899 (to be issued).

? DP 900

13. Previous progress reports in this series are:

DP-232	DP-395	DP-485	DP-575	DP-665	DP-755	DP-845
DP-245	DP-405	DP-495	DP-585	DP-675	DP-765	DP-855
DP-265	DP-415	DP-505	DP-595	DP-685	DP-775	DP-865
DP-285	DP-425	DP-515	DP-605	DP-695	DP-785	DP-875
DP-295	DP-435	DP-525	DP-615	DP-705	DP-795	DP-885
DP-315	DP-445	DP-535	DP-625	DP-715	DP-805	DP-895
DP-345	DP-455	DP-545	DP-635	DP-725	DP-815	DP-905
DP-375	DP-465	DP-555	DP-645	DP-735	DP-825	
DP-385	DP-475	DP-565	DP-655	DP-745	DP-835	